

This is an Open Access document downloaded from ORCA, Cardiff University's institutional repository: <https://orca.cardiff.ac.uk/id/eprint/162071/>

This is the author's version of a work that was submitted to / accepted for publication.

Citation for final published version:

Li, Amber Xinyu, Martin, Tracey A. , Ye, Lin , Ruge, Fiona, Sanders, Andrew J. , Khan, Elyas, Dou, Q. Ping, Davies, Eleri and Jiang, Wen G. 2023. Striatins and the STRIPAK complex partners in the clinical outcome of patients with breast cancer and responses to drug treatment. Chinese Journal of Cancer Research 35 , pp. 365-385. 10.21147/j.issn.1000-9604.2023.04.04

Publishers page: <https://doi.org/10.21147/j.issn.1000-9604.2023.04....>

Please note:

Changes made as a result of publishing processes such as copy-editing, formatting and page numbers may not be reflected in this version. For the definitive version of this publication, please refer to the published source. You are advised to consult the publisher's version if you wish to cite this paper.

This version is being made available in accordance with publisher policies. See <http://orca.cf.ac.uk/policies.html> for usage policies. Copyright and moral rights for publications made available in ORCA are retained by the copyright holders.



Striatins and the STRIPAK complex partners in the clinical outcome of patients with breast cancer and responses to drug treatment

Amber Xinyu Li¹, Tracey A. Martin¹, Lin Ye¹, Fiona Ruge¹, Andrew J. Sanders^{1,2}, Elyas Khan³, Q. Ping Dou^{1,3}, Eleri Davies⁴, Wen G. Jiang^{1,*}

1 Cardiff University School of Medicine, Heath Park, Cardiff, CF14 4XN, UK. LiX193@cardiff.ac.uk (A.X.L.), MartinTA1@cardiff.ac.uk (T.A.M); YeL@cardiff.ac.uk (Y.L.) Ruge@cardiff.ac.uk (F.R.); sandersaj1@cardiff.ac.uk (A.J.S.); DouQ1@cardiff.ac.uk (Q.P.D.); Jiangw@cardiff.ac.uk (W.G.J.)

2 School of Natural and Social Science, University of Gloucestershire, Francis Close Hall, Swindon Road, Cheltenham, GL50 4AZ, UK. asanders2@glos.ac.uk (A.J.S.)

3 Karmanos Cancer Institute, Department of Oncology, School of Medicine, Wayne State University, Detroit, MI 48201, USA. elyaskhan882@gmail.com [E.K.]; doup@karmanos.org (Q.P.D.),

4 Wales Breast Centre, Cardiff and Vales University Health Board, University Llandough Hospital, Cardiff CF64 2XX, UK. Eleri.Davies8@wales.nhs.uk (E.D.)

* Professor Wen G Jiang, Cardiff China Medical Research Collaborative (CCMRC), Division of Cancer and Genetics (DCG), Cardiff University School of Medicine, Henry Wellcome Building, Heath Park, Cardiff, UK, CF14 4XN; Tel: +44 2920 687065; E-mail: jiangw@cardiff.ac.uk

Abstract:

Background. Striatins family (STRNs), which contains three multi-domain scaffolding proteins, are cornerstones of the striatins interacting phosphatase and kinase (STRIPAK) complex. Although the role of the STRIPAK complex in cancer has become recognized in recent years, its clinical significance in breast cancer has not been fully established. **Methods.** Using a freshly frozen breast cancer tissue cohort containing both cancerous and adjacent normal mammary tissues, we quantitatively evaluated the transcript-level expression of all members within the STRIPAK complex along with some key interacting and regulatory proteins of STRNs. The expression profile of each molecule and the integrated pattern of the complex members were assessed against the clinical-pathological factors of the patients. TCGA dataset was used to evaluate the breast cancer patient's response to chemotherapies. Four human breast cancer cell lines, MDA-MB-231, MDA-MB-361, MCF-7, and SK-BR-3, were subsequently adopted for in vitro work. **Results.** Here we found that high-level expression of STRIP2, calmodulin, CCM3, MINK1 and SLAMP were respectively associated with shorter overall survival (OS) of patients. Although the similar pattern observed for STRN3, STRN4 and a contrary pattern observed for PPP2CA, PPP2CB and PPPR1A were not significant, the integrated expression profile of STRNs group and PPP2 group members constitutes a highly significant prognostic indicator for OS ($p < 0.00001$, HR=2.1 (95%CI 1.36-3.07)) and DFS ($p = 0.003$, HR=1.402 (95%CI 1.12-1.75)). Reduced expression of STRN3 has an influence on the biological functions including adhesiveness and migration. In line with our clinical findings, the breast cancer cells responded to STRN3 knockdown with changes in their chemo-sensitivity, of which the response is also breast cancer subtype dependent. **Conclusion.** Our results suggest a possible role of the STRIPAK complex in breast cancer development and prognosis. Among the members, the expression profile of STRN3 presents a valuable factor for assessing patients' responses to drug treatment.

Keywords: Striatins, STRN3, STRIPAK, breast cancer; prognosis; chemoresistance

Running title: Striatins and STRIPAK in breast cancer

1. Introduction

The investigation on the STRNs' family arose from two decades ago. Muro et al. have identified a protein, which is now known as striatin-3 (STRN3, or SG2NA), during the S and G2 phase of the cell cycle by using antibodies acquired from cancer patient [1]. While this study was being conducted, another research, which speculated the activities of adenylyl cyclase at the synapses, had coincidentally

discovered a WD-repeat family protein, called striatin (STRN), highly expressed at the dendritic sites in rat brain [2]. The final member constituting the STRNs family, zinedin, was discovered in 2000 and was renamed later as striatin-4 (STRN4) [3]. The three STRNs are homologous proteins that contain similar number of amino acids and possess identical interacting domain structure including a caveolin-binding domain, a coiled-coil region, a calmodulin (CaM, or CALM1) binding domain and a WD-repeat domain. Consistent with the presence of those domains, STRNs appear to associate with caveolin-1 and calmodulin in a Ca^{2+} dependent manner [4, 5]. It is now established that the members within the STRNs family are both cytosolic and membrane-bound proteins, and recently STRNs have also been suggested to function as cell adhesion regulators at both adherens junctions and tight junctions in epithelial cells [3, 6]. Although the full functions of STRNs were not entirely clear, the findings that they interacted with protein phosphatases, namely PP2A (protein phosphatase 2A) (coded by the *PPP2CA* gene) and PP2B (protein phosphatase 2B) (coded by the *PPP2CB* gene) indicated their role in regulating the phosphatases and phosphorylation events.

In terms of signalling partners, perhaps the most important discovery is that STRNs, particularly STRN3 is a cornerstone protein for the STRIPAK complex (the striatin-interacting phosphatases and kinases). The STRIPAK complex contains a rather large number of subunit proteins sufficiently linked by STRN3 via their coiled duplex domain, which is a region serves as platform allowing other partners to dock [8, 9]. Some of the well-known STRIPAK members are STRN3, calmodulin, PP2A, caveolin, MOB4 and GCKIII. While in recent years, CCM3 (cerebral cavernous malformations 3, or PDCD10 (programmed cell death protein 10)), SLMAP (sarcoma associated protein), STRIP1 (striatin interacting proteins 1, or FAM40A (family with sequence similarity 40 member A)), STRIP2 (striatin interacting proteins 2, or FAM40B), PP2CB, PPP2R1A (protein phosphatase 2A regulatory subunit A), CTTNBP2 (cortactin binding protein 2), MST1 (macrophage stimulating-1 or hepatocyte growth factor like protein (HGFL)), SIKE1 (suppressor of IKK epsilon) and MINK1 (misshapen like kinase 1) were also reported to be closely or loosely associated with the STRIPAK complex and are also regarded as the STRIPAK partners [10-12]. The functions of STRNs and STRIPAK are not entirely clear but with the number and complexity pattern of the interacted partners, one can predict that their function would be complex and diverse.

STRNs are known to bind with caveolin and calmodulin, contributing to T-cell proliferation and Ca^{2+} dependent tissue activation [5]. Gordon et al. has claimed that STRN is able to orchestrate the regulation of CCM3 and MST3 by PP2A [13]. SLMAP, as part of the STRIPAK complex has also been implicated in cell-cycle control [14]. The recent study conducted by Lahav-Ariel et al., has shown that STRN may be poly-ADP-ribosylated following interaction with Tankyrase 1 (TNKS1) [6]. STRN and MOB4 (Mps one binder kinase activator family member 4) together could coordinate the Wnt signalling pathway and play a role in embryonic development [15]. STRIPAK is also involved in the Hippo signalling event and the Hippo-STRIPAK complex could act on DNA double-stranded break repair and genomic stability [16, 17].

In colon epithelial cells, STRN was found to colocalise with APC (adenomatous polyposis coli), while targeting either STRN or APC impeded the tight junctional functions in these cells [18]. Additionally, knocking down STRN inhibited cell migration of endothelial cells [20]. This regulation of adhesion by STRN seems to involve both tight junctions and adherens junctions and possibly the interactive relationship between the two important cell adhesion and permeability structures [6]. Moreover, the anchoring of the membrane localized ER mediated by its interaction with STRN has been suggested to facilitate breast cancer cell survival, proliferation and endocrine resistance [21].

The role of the STRIPAK complex in cancer is becoming recognized in recent years. In clinical cancer and database analyses, STRIPAK was thought to be a possible oncogenic complex in liver hepatocellular carcinoma (HCC) and renal clear cell carcinoma (RCCC) [22]. STRN4 was found to aberrantly affect liver HCC cells and STRN4 suppression resulted in reduction of tumorigenicity of these liver cancer cells [24]. Ito et al., have recently reported the appearance of anti-STRN4 antibody

in patients with oesophageal cancer and the antibody levels appear to have both diagnostic and prognostic values for oesophageal squamous cell carcinoma (SCC) [25]. In thyroid cancer, it has been shown that the complex gene rearrangement resulted in formation of a STRN-ALK kinase fusion protein, allowing ALK activation and promoting tumour formation [31]. Qiu et al. have shown that STRIP2 is also an oncogenic player for lung adenocarcinoma cells [29].

There are several pathways that STRNs participate in the regulation of cellular functions in cancer cells. In pancreatic cancer cells, STRN4 knockdown suppressed cell growth and invasion [26]. Of a particular interest is the connection between STRNs and cancer cells response to drug treatment. Knocking down STRN4 in pancreatic cancer cells increased the sensitivity of cells to gemcitabine [26]. In breast cancer cell line, MCF-7, targeting the functional form of STRN3 protein by truncated protein confers EMT transformation of the cells [30].

The link between STRNs and drug response in breast cancer has not been fully explored. Breast cancer tissues have been shown to possibly express different variant form of the STRN3 proteins, which in turn may involve in diverse signalling events [38]. There is a good reason that STRNs and STRIPAK members may play a role in breast cancer. STRNs family members have been shown to serve as scaffolds for formation of protein complexes between PP2A and oestrogen receptor, ER α [39, 40]. Oestrogen, via ER α , is a central player in the development and progression of breast cancer, a connection established for almost a century. Beyond this connection, the multiple biological functions played by STRNs and STRIPAK partners also suggest that the STRIPAK complex may play an important role in breast cancer.

Most of the previous studies have examined individual members of the STRIPAK family. There have been no reports on the comprehensive analysis of the STRIPAK complex members in any cancer type. Therefore, the present study collectively explored the expression of a cohort of STRIPAK complex members in breast cancer and examined the clinical and potential therapeutic values of these molecules.

2. Materials and Methods

2.1. Cell lines

Four human breast cancer cell lines, namely MDA-MB-231, MDA-MB-361, MCF-7, and SK-BR-3 were obtained from ATCC (LGC standard, England) and cultured in Dubecco's Modified Eagle Medium (DMEM). The culturing medium was supplemented with 10% fetal calf serum (FCS) (Sigma-Aldrich, Dorset, UK) and 1X antimicrobial solutions (Sigma-Aldrich, Dorset, UK). Cells were cultured in an incubator with pH level of 7.3, at 95% humidity, 5% CO₂ and 37°C.

2.2. Drugs and antibodies

Two purified chemo-drugs, Paclitaxel and Docetaxel purchased from Sigma-Aldrich (Dorset, UK) were dissolved and further diluted to a desired concentration. Antibodies used in protein blotting were mouse anti-human GAPDH (SC-32233) (Santa Cruz Biotechnologies Inc., CA, USA), rabbit anti-human STRN (PA5 -53576), Thermofisher, Oxford, England, UK), and rabbit anti-STRN3 (GTX65851), GeneTex, Ely, England, UK.

2.3. Tissue cohort

Freshly frozen breast cancer tissue cohort contains both cancerous and adjacent background mammary tissues was used as previously reported [41]. Written informed consent was required and obtained from patients, and a follow-up study with median follow-up period of 120-months was conducted after the surgery. The samples were collected under ethical approval (Bro Taf Health Authority; ethics approval number 01/4303 and 01/4046).

2.4. PCR and QPCR

Gene transcripts of STRNs and the STRIPAK partners were evaluated by real time quantitative PCR by employing the Amplifluor Molecular Beacon system. Reactions were prepared in a MicroAmp fast Optical 96-well plate (Fisher Scientific UK, Leicestershire, UK) using primers specific to the molecule of interest (see Supplement-1). In addition to unknown samples, reactions were prepared for a known standard that was run alongside the unknown samples on a StepOne Plus qPCR system (Fisher Scientific UK, Leicestershire, UK). Following the run, relative copy numbers of the samples were calculated as part of the systematic analysis, in accordance with the standard curve.

2.5. Breast cancer cell models

Four breast cancer cell lines, MDA-MB-231, SKBR3, MCF-7 and MDA-MB-361, representing different subtypes of breast cancer, were used to create sublines with STRN and STRN3 knockdown by following the manufacturer's instructions. Lentiviral shRNA targeting human STRN (SC-37649v) and STRN3 (SG2NA) (SC-37647v) and siRNA targeting STRN (SC-37649) and STRN3 (SG2NA) (SC-37647) were purchased from Santa Cruz Biotechnologies Inc. Each knockdown included three sets of siRNAs. The sequences of the three sets for STRN were: Set-A: Sense- CGGUGAAGAUCGAGAUACAAtt and antisense-UGUAUCUCGAUCUUCACCGtt; Set-B: Sense- CAGACUCACUAAACUUAUGAtt and antisense-UCAUAAGUUAGUGAGUCUGtt; and set-C: Sense- CAAGGGAUAUACAAGCAUUt and antisense-AAUGCUUGUAUAUCCCUUGtt. The sequences of the three sets for STRN3 were: set-A: sense-GAAUGGGCUGAACCAUAAtt and antisense-UUAUUGGUUCAGCCCAUUCtt; Set-B: sense-CCAGUGUAGAUCCAUAUGAtt and antisense-UCAUAUGGAUCUACACUGGtt; and set-C: sense-GUCUAGCAGUAGAUCCUAAAtt and antisense: UUAGGAUCUACUGCUAGACtt. For shRNA lentiviral transduction, polybrene was used with the viral stock to transduce breast cancer cells. Puromycin was used at 2µg/ml to select the stable knockdown cells and at 0.2µg/ml to maintain the stability of the transfected cells.

2.6. SDS PAGE and protein blotting

Proteins were extracted from cultured cells with RIPA buffer and quantified by BioRad protein quantitation kit (Bio-Rad Laboratories, Hertfordshire, UK.). The samples were treated with 2x Laemmle sample buffer, boiled at 100°C for 5mins and then loaded to 8% (for STRN and STRN3) or 10% (for GAPDH) SDS PAGE gel for electrophoresis. Semi-dry transfer system was then adopted for protein transfer from the gel onto the PVDF member which was pre-activated by methanol. 10% milk was used for membrane blocking. The blots were respectively incubated with the primary antibody against STRN, STRN3 and GAPDH, followed by further exposure to the HRP conjugated secondary antibody before visualised using EZ-ECL solution (Geneflow Ltd., Litchfield, UK).

2.7. Dynamic monitoring of cell behaviour with electric cell-substrate sensing (ECIS)

Wild type (WT) cancer cells, the cells with STRN and STRN3 knockdowns, were tested using ECIS to monitor cell's biological responses following the genetic modification. Cell adhesiveness and migration was monitored according to the methods previously reported [42-44]. Briefly, the respective cells were added into the 96 well microelectrode array 96W1E plate that was pre-treated for optimising electrical conductivity. The plate was mounted onto the ECIS Z-Theta unit, purchased from Applied Biophysics Inc., immediately after the cells were seeded. Cell adhesiveness was monitored for up to 6 hours over all frequencies between 1,000Hz to 64,000Hz. For cell migration assay, the array wells were electrically wounded at 2000mA for 20 seconds to create cell free wounds over the gold coated electrodes. The migration pace of the cells was immediately monitored, again over the same range of frequencies for up to 20 hours.

2.8. Cell matrix adhesion assays

Cell matrix adhesion assay was performed on 96-well plate that was pre-coated with Matrigel (FisherScientific) (0.5µg/well). Forty thousand cells prepared in DMEM were subjected into each well

followed by incubation at 37°C with 5% CO₂. After 40mins, non-adherent cells were carefully washed with PBS and the adhered cells were fixed with 4% formalin, stained with 0.5% (w/v) crystal violet, and counted under microscope at a 20X magnification. Each application was repeated 6 times and two photos were randomly taken for each well. The cell number quantification was performed by ImageJ.

2.9. Patients' response to chemotherapies and evaluation

Here, we used a comprehensive public database which contain breast cancer patients with their therapeutic options recorded [45]. The database took the approach of ROC (receiver operating characteristic curve), allowing classification of patients' sensitivity to a therapy. Here, the AUC (Area Under the Curve) values and the statistical value for sensitivity to treatment were recorded. Additionally, the levels of the respective gene expression of the gene of interest were also displayed together with their statistical power (by Mann-Whitney U test).

2.10. In vitro drug sensitivity tests

Cells were seeded into 96 well plates and treated with 1:10 serial-diluted drugs. The concentrations of the drugs were respectively chosen based on their known IC₅₀ and previous studies. After 72 hours, the cells were fixed with 4% formalin, stained with 0.5% crystal violet and extracted with 10% acetic acid after washing. The absorbance was measured at 595 nm using a spectrophotometer to detect their respective cell densities. The percentage drug toxicity was calculated as follow: $\text{Percentage drug toxicity} = [(\text{Absorbance in untreated well} - \text{Absorbance in drug treated well}) / \text{Absorbance in untreated well}] \times 100$. The scatter plots of percentage toxicity versus drug concentration were plotted, and the best fit curve was used to calculate the respective IC₅₀ value.

2.11. Statistical methods

Statistical analyses were carried out using SPSS (version 27.0). Groupwise comparisons were conducted by Kruskal-Wallis test and ANOVA where applicable. Integrated informatics was also tested using the Bayesian models. Pairwise comparisons were done by Mann-Whitney U test as indicated in the text. Kaplan-Meier method and log rank test were used to run survival analysis. Univariate and multivariate analyses were conducted using Cox regression model. Classification analysis was achieved by the Receiver operating characteristic (ROC) method.

3. Results

3.2. Expression profile of STRNs and STRIPAK complex partners in breast cancer

We quantified the transcript levels of the known STRIPAK partner molecules including all STRNs, STRIPs, Calmodulin caveolin, CCM3 (PDCD10), SIKE1, MINK1, MOB4, PPP2CA and PPP2CB, PPP2R1A and PPP2R4, MST1, TNKS1 and TNKS2 in mammary tissues of the cohort. Table-1 summarises the transcript levels of these genes in tissues and in subgroups of the patients. All three STRNs members were expressed at transcript level in mammary tissues and cancer tissues, while only STRN had a markedly higher transcript level expression in tumour than normal tissue ($p < 0.01$). Both of the STRNs binding proteins, calmodulin and caveolin, exhibited increased expression in the tumour tissue, yet the differences observed for calmodulin did not reach statistical significance. STRNs were not associated with Nottingham prognostic index (NPI). The expression of some of the other STRIPAK member, namely MST1 was strongly associated with the NPI ($p < 0.05$). STRIP1, PP2R1A and PP2R4 were significantly elevated in high grade tumours ($p < 0.05$) (Table-1). STRIP2 and MST1R were seen to significantly differ between disease free and patients with breast cancer related incidence (Table-1). The study also examined the expression levels of the STRIPAK partners in relation to ER and Her2 status and as shown in Table-1, calmodulin was significantly different in high and low ER tumours. Likewise, TNKS2 and STRIP2 also significantly differ in different Her2 groups.

Table-1a. Expression of striatins and STRIPAK partners in mammary tissues and breast cancer tissues of Cardiff cohort.

Category	Subgroup	n=	STRN	STRN3	STRN4	STRIP1	STRIP2	Calmodulin	PPP2CA	PPP2CB	PPP2R1A	PPP2R4
Tissue type	Normal	33	12.05(3.96-35.03)	0.49(0.11-4.21)	85.3(32.4-168.1)	4573(2156-45892)	25857(1662-118966)	3.18(0.72-22.5)	0.3(0.1-3.2)	0(0-3)	1.9(0.6-3.3)	0.00001(0-0.00037)
	Tumour	127	57(14-288) ^a	0.75(0.02-10.09)	84.5(14.9-335.6)	4156(2495-8175)	10232(1750-49386)	5.7(0.4-44.6)	0.5(0.1-3)	1(0-7)	1.58(0.5-4.28)	0.00003(0-0.00027)
Nottingham Prognostic Index (NPI)	Good	68	63(12-254)	0.5(0-12.8)	78.9(4.9-245)	4192(2562-7838)	12908(1728-43916)	2.9(0.1-49.6)	0.6(0.1-4.4)	1(0-46)	1.52(0.5-4)	0.00003(0-0.00029)
	Moderate	38	85(15-866)	0.9(0.1-10)	120(32.3-606.9)	4553(2440-9838)	4761(120-109529)	12(1.8-45.4)	0.22(0.04-7.37)	0.9(0.2-3.1)	1.862(0.409-4.352)	0.00005(0-0.00032)
	Poor	16	49.7(6.6-248.8)	1.07(0.03-13.21)	91.8(33.5-331.8)	3326(1906-15825)	9787(768-213921)	2.62(0.25-17.95)	0.69(0.18-1.35)	0(0-1)	1.869(0.657-3.836)	0.0001(0-0.00018)
Grade	Grade-1	24	25(1-629)	0.16(0-10.13)	50(2-585)	3209(2210-4545)	15580(2221-94997)	2(0-35)	0.3(0.1-4.5)	1.3(0.2-2.7)	0.597(0.121-2.084)	0.00002(0-0.00018)
	Grade-2	43	94(26-557)	0.5(0.1-14.9)	102(10-399)	3708(1673-7023)	9526(411-47310)	2(0.1-52.5)	0.32(0.04-1.68)	1(0-14)	2.101(1.046-5.55) ^d	0.00002(0-0.00014) ^d
	Grade-3	58	49.7(7.1-209.8)	1.1(0.2-7.5)	84.8(35.3-238.2)	6101(2909-16558) ^d	8105(1854-83647)	11.1(1.8-44.6)	0.82(0.11-5.22)	1(0-11)	1.37(0.52-4.32)	0.00007(0-0.00034) ^d
Clinical outcome	Disease free	90	49(7-455)	0.8(0-12.5)	96.8(14.7-357.8)	3914(2577-7390)	12543(2031-68358)	6.3(0.4-46.2)	0.5(0.1-2)	1(0-6)	1.49(0.5-4.02)	0.00002(0-0.00022)
	With Metastasis	7	73.5(25.1-212.5)	0.8(0.16-7.77)	85(55.2-125.2)	2868(1684-6967)	199(31-1972) ^e	5.4(0-55.9)	1.8(0.1-8.2)	1.4(0.4-170.6)	1.88(1.14-9.6)	0.00042(0.00001-0.00067)
	Died of BrCa	16	149(4-667)	0.89(0.04-7.56)	99.9(11.6-463.4)	7150(2466-19400)	8148(701-32499)	10.2(0.8-40.7)	0.18(0.06-2.1)	1(0-8)	2.6(0.5-7.7)	0.00008(0-0.00014)
	All Incidence	28	80.2(32-250.7)	0.77(0.04-6.43)	81.2(28.3-270.2)	5685(1811-9074)	2537(278-29621)	7.5(0.4-44.6)	0.66(0.08-2.87)	1.4(0.2-8.4)	2.1(1.14-7.73)	0.00008(0-0.00031)
Nodal status	Positive	54	55(15-554)	1(0.1-10.2)	119.8(33.2-420.6)	4545(2483-10050)	8127(701-119800)	9.7(0.9-43.2)	0.4(0.08-2.27)	1(0-2)	1.869(0.518-4.237)	0.00005(0-0.0003)
	Negative	68	63(12-254)	0.5(0-12.8)	78.9(4.9-245)	4192(2562-7838)	12908(1728-43916)	2.9(0.1-49.6)	0.6(0.1-4.4)	1(0-46)	1.52(0.5-4)	0.00003(0-0.00029)
ER status	Negative	75	57.4(14.3-287.7)	1(0-10.7)	85(19.6-305.2)	3337(2483-6189)	14070(1868-47039)	11.1(1.5-51.3)	0.5(0.1-4.2)	1(0-8)	1.585(0.525-3.836)	0.00004(0-0.0003)
	Positive	38	59(11-2129)	0.5(0-6.5)	78.9(3.9-493.7)	5055(2528-8209)	6278(793-55289)	2.1(0-17.9) ^f	0.55(0.07-3.8)	1(0-6)	2.1(0.45-6.42)	0.00005(0-0.00014)
Her2	Her2(-)	57	52(7-586)	1.1(0.1-15.1)	102.1(16.4-398.5)	4545(2184-8001)	33053(7107-101396)	5.3(0.5-29.6)	0.8(0.2-3.3)	1(0-6)	1.49(0.48-3.84)	0.00004(0-0.00027)
	Her2(+)	55	81(29-254)	0.75(0.02-7.14)	84.5(13.8-311.9)	3632(2355-8786)	5958(806-30208) ^g	12(0.4-49.1)	0.33(0.08-3.23)	1(0-8)	1.71(0.5-4.51)	0.00002(0-0.00032)

Table-1b. Expression of striatins and STRIPAK partners in mammary tissues and breast cancer tissues of Cardiff cohort.

Category	Subgroup	n=	CCM3	MINK1	MOB4	SIKE1	SLMAP	MST1 (HGFL)	MST1R (RON))	Caveolin	TNKS1	TNKS2
Tissue type	Normal	33	6790(3773-15861)	5948(2561-9834)	20235(9388-25369)	2153(499-3581)	4453(2161-9633)	7(0-412)	0(0-179)	0.164(0.047-0.363)	2.26(0.87-6.03)	0.01(0-0.7)
	Tumour	127	6183(1734-23717)	5525(1996-17477)	19852(7196-38318)	1995(971-4135)	3243(1378-17215)	2(0-349)	0(0-1488)	0.45(0.09-2.49)	5.8(0.5-22.7)	0.01(0-3.22)
Nottingham Prognostic Index (NPI)	Good	68	6832(1827-23843)	5343(1655-16941)	18779(7947-33941)	1907(984-3997)	2904(1252-16639)	0(0-466)	0(0-787)	0.358(0.078-2.14)	1.93(0.31-16.92)	0.09(0-4.55)
	Moderate	38	7508(1284-34305)	6328(2014-28532)	19848(4955-41073)	2499(1338-5834)	4575(1445-17335)	3(0-487)	0(0-160) ^b	0.68(0.12-2.53)	7.9(1-26.7)	0(0-0.9)
	Poor	16	4619(2687-24503)	5678(2431-23419)	31648(16480-42687)	948(463-2884)	9459(3121-44016)	1(0-249)	350(0-41341) ^c	0.78(0.1-7.38)	12(1-44)	0(0-2.57)
Grade	Grade-1	24	3688(1613-13758)	4476(1148-13647)	14373(3902-25883)	2023(1224-5861)	3243(1749-25592)	0(0-135)	0(0-1211)	1.3(0.1-2.7)	3.6(0.2-9.4)	0(0-2.61)
	Grade-2	43	5499(1048-20152)	5905(1348-17857)	18203(5514-33671)	3063(1569-4265)	2603(882-9366)	9(0-737)	0(0-76)	0.597(0.093-2.69)	2.57(0.32-17.71)	0.14(0-4.61)
	Grade-3	58	7049(2832-28673)	5525(2106-21790)	26244(13390-40611)	1601(553-2593)	6690(1772-36975)	0(0-328)	4(0-9011)	0.37(0.08-1.5)	9.9(0.9-36)	0(0-2.95)
Clinical outcome	Disease free	90	5741(1892-24631)	5658(2205-16122)	20591(7196-38318)	2257(1295-3747)	2805(1279-15751)	14(0-494)	0(0-212)	0.47(0.1-2.55)	6.2(0.5-17.7)	0.01(0-3.55)
	With Metastasis	7	3607(734-4230)	4353(2673-5150)	22548(8688-37321)	2800(592-5278)	2802(882-3037)	0(0-777)	0(0-101)	0.05(0.01-0.78)	15.2(3.3-64.2)	0.002(0-0.18)
	Died of BrCa	16	11445(3734-47878)	15408(1529-28364)	35484(18815-41867)	1086(401-5153)	7772(1916-44016)	0(0-51)	9020(0-41341)	0.3(0.03-1.83)	11(1-44)	0.06(0-18.82)
	All Incidence	28	6959(1245-24352)	4379(1909-26160)	31648(10839-41073)	1623(414-4377)	6883(1836-31760)	0(0-51)	39(0-17005) ^e	0.23(0.03-1.83)	11.9(0.9-64.2)	0.01(0-2.57)
Nodal status	Positive	54	6652(1875-24807)	5905(2303-26199)	27954(8118-41469)	2393(1290-4283)	6883(1567-29843)	2(0-320)	1(0-4320)	0.68(0.12-2.63)	9.2(0.9-31)	0(0-1.18)
	Negative	68	6832(1827-23843)	5343(1655-16941)	18779(7947-33941)	1907(984-3997)	2904(1252-16639)	0(0-466)	0(0-787)	0.358(0.078-2.14)	1.93(0.31-16.92)	0.09(0-4.55)
ER status	Negative	75	4667(1908-20436)	5736(2495-16532)	25332(14048-37111)	1823(1290-3090)	2853(1395-14034)	14(0-698)	1(0-2315)	0.31(0.07-1.98)	5.14(0.48-18.42)	0.01(0-3.26)
	Positive	38	7265(1428-24809)	4405(765-21412)	14850(5222-40614)	2084(616-5301)	4351(1306-27238)	0(0-70)	0(0-1005)	0.777(0.173-2.53)	5.3(0.8-23.6)	0.01(0-3.68)
Her2	Her2(-)	57	4817(1899-24173)	6116(3052-16218)	20591(11843-36248)	2522(984-5112)	3690(1388-17456)	9(0-447)	0(0-1312)	0.75(0.1-2.17)	1.5(0.3-18.4)	0.01(0-3.89)
	Her2(+)	55	7472(1657-25436)	4379(1491-20523)	19852(6181-39955)	1826(744-3734)	3093(1333-19952)	0(0-296)	0(0-2165)	0.36(0.07-1.83)	8.3(1.3-39)	0(0-3.36) ^g

Note: Shown are Median (interquartile range). Mann-Whitney U tests were conducted and statistical significance was reached by comparing between the groups. ^a p<0.05 vs normal; ^b p<0.05 vs good prognosis; ^c p<0.05 vs moderate prognosis; ^d p<0.05 vs Grade-1; ^e p<0.05 vs disease free; ^f p<0.05 vs ER negative; ^g p<0.05 vs Her2 negative;

Table-2. STRIPAK and patients' OS and DFS, Cardiff data by Cox Regression

	OS		DFS	
	P value	HR	P value	HR
STRN	0.434	1.804 (0.411-7.918)	0.260	2.306 (0.539-9.871)
STRN3	0.178	2.031 (0.724-5.700)	0.384	1.465 (0.621-3.456)
STRN4	0.196	3.789 (0.504-28.492)	0.248	2.352 (0.551-10.038)
STRIP1	0.053	3.018 (0.984-9.254)	0.249	1.853 (0.649-5.292)
STRIP2	0.014	4.388 (1.349-14.267)	0.265	1.781 (0.646-4.913)
Calmodulin	0.019	4.384 (1.269-15.149)	0.055	2.489 (0.981-6.316)
PPP2CA	0.063	0.414 (0.163-1.050)	0.069	0.468 (0.206-1.061)
PPP2CB	0.110	0.471 (0.187-1.186)	0.105	0.509 (0.224-1.153)
PPP2R1A	0.079	0.436 (0.173-1.100)	0.073	0.473 (0.208-1.073)
PPP2R4	0.590	1.292 (0.509-3.278)	0.752	1.141 (0.503-2.589)
CCM3	0.032	4.003 (1.128-14.205)	0.488	1.381 (0.555-3.437)
MINK1	0.011	3.749 (1.356-10.361)	0.146	2.053 (0.779-5.410)
MOB4	0.010	4.598 (1.441-14.676)	0.075	2.460 (0.915-6.613)
SIKE1	0.115	3.056 (0.763-12.246)	0.136	2.467 (0.752-8.086)
SLAMP	0.035	3.496 (1.093-11.176)	0.178	2.033 (0.723-5.714)
MST1 (HGFL)	0.441	0.646 (0.213-1.964)	0.358	0.628 (0.233-1.693)
MST1R (RON)	0.415	1.473 (0.581-3.735)	0.285	1.569 (0.687-3.580)
Caveolin	0.674	0.816 (0.315-2.110)	0.303	0.648 (0.283-1.481)
TNKS1	0.093	5.666 (0.748-42.94)	0.054	7.253 (0.970-54.222)
TNKS2	0.261	1.854 (0.633-5.431)	0.692	1.194 (0.497-2.870)

3.3. STRNs and STRIPAK, the connection to the clinical outcome of the patients

The expression levels of transcripts of all the STRIPAK partners were then analysed against the survival of the patients by using the ROC method. Using the most favorable cutoff value generated, patients were divided into groups with high- or low-level expression and were analysed against both overall survival (OS) and disease-free survival (DFS) by using the Kaplan-Meier method. Cox regression model was also applied to calculate the hazard ratio (HR) of each molecule against OS and DFS. As shown in Table-2, expression of STRIP2, Calmodulin, CCM3, MINK1, MOB4, SLAMP and to some degree STRN3, STRN4, PPP2CA, PPP2CB, PPP2R1A had marked association with the survivals of the patients.

High-level expressions of *STRN3*, *STRN4* and *CALM* were associated with shorter overall survival (OS) of the patients and together they formed a poor prognostic indicator ($p=0.034$, $HR=1.7$). STRN had little impact on clinical outcomes. The other components of the core STRIPAK complex had shown a clear contrasted trend, in which high levels of *PPP2CA*, *PPP2CB* and *PPP2R1A*, but not *PPP2R4*, were seen in patients with significantly longer OS and together form a favourable prognostic indicator ($p=0.034$, $HR=0.685$). The transcript level expression of the aforementioned molecules did not show a significantly correlation with DFS of the breast cancer patients except for Calmodulin and TNKS1 which showed marginal p value with a high HR (Table-2).

3.4. Derivation of a STRNs/STRIPAK gene signature in assessing the survival of the patients

Integration of the core molecules of the STRIPAK complex constitutes a highly significant prognostic indicator for OS ($p<0.00001$, $HR=2.1$ (95%CI 1.36-3.07)) and DFS ($p=0.003$, $HR=1.402$ (95%CI 1.12-1.75)) (Figure-1). The predictive value of the integrated profile is independent of other clinical, pathological and hormone receptor status in multivariate analyses with OS ($p<0.0001$, $HR=3.861$) and for DFS ($p<0.001$, $HR=2.055$ (95%CI 1.36-3.07)) (Table-3).

The expression pattern of the shortlisted STRIPAKs were also tested using ROC method (Figure-1A). There is a significant predictive value in predicting the OS ($AUC=0.836$, $p=6.35\times 10^{-12}$). The signature was additionally tested using the Bayesian model that has returned a Bayes factor at 0.000205

with a mode factor at 3.2232, strongly suggesting that the signature has a strong value to predict the survival outcome of the patients.

Patients were then stratified into two groups based on their expression pattern of the signature. The stratification showed a highly significant value in predicting the overall survival ($p=0.00003$) (Figure-1B). Independent analysis of this connection by Bayesian Loglinear model returned with a Bayes factor of 0.00006285 and mode factor 5.4571, again being highly supportive of the findings. To evaluate the significance of the independency of the signature in predicting the overall survival, we carried out multivariate analysis together with other clinical and indeed hormone receptor-based subtype analysis. As shown in Table-3, the STRIPAK signature presents a significant prognostic value ($p<0.001$) independent from other clinical factors and hormone receptor status of patients.

The signature has also significantly correlated with the disease-free survival ($p=0.003$) (Figure-1C), supported by the independent Bayesian model with Bayes factor at 0.258. Likewise, when patients were divided into three groups, it also predicted a group with outstanding survival and poor survival. We further stratified the patients with conventional biomarkers namely ER and Her-2 status. As shown in Figure-1, the signature identified those with worst outcome who had ER negative, Her-2 positive and most stringly ER(-)/Her-2(+) tumours. It is also noteworthy that the signature has not improve the prediction of outcome in TNBC tumours (Figure-1F2).

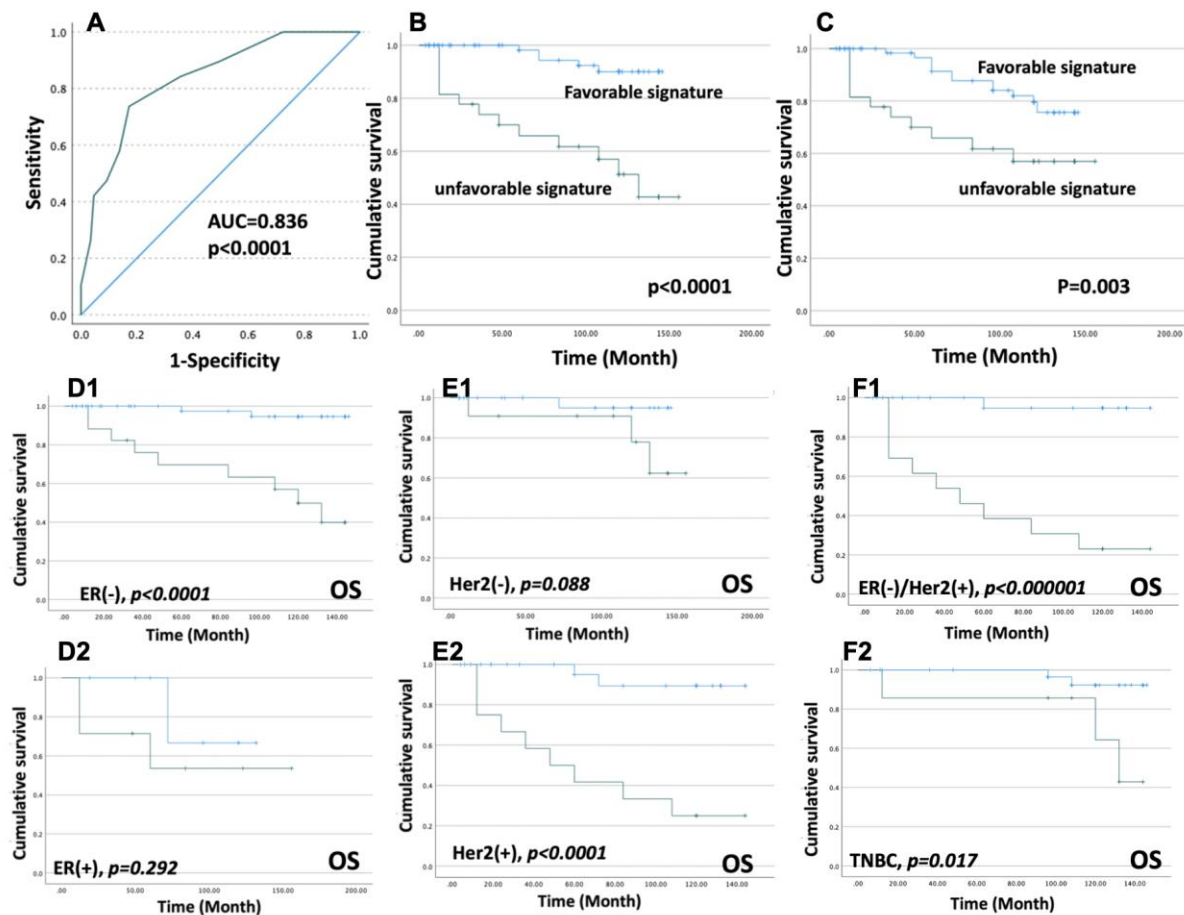


Figure-1. Integrated STRN and other core STRIPK members and the prediction of patient survival. The expression pattern of the shortlist STRIPAKs are tested using ROC method (A). There is a significant predictive value in predicting the OS (AUC=0.836). Patients were then stratified into two groups based on their expression pattern of the signature. The stratification showed a highly significant value in predicting the overall survival ($p<0.0001$) (B) and disease-free survival (C). The signature identified those patients who had worst outcome in ER negative tumours (D1), Her-2 positive tumours (E2) and more profoundly in ER(-)/Her2(+) tumours (F1), whereas it had little additional value for ER(+) tumours (D2), Her-2 negative tumours (E1) and TNBC tumours (F2).

Table-3. Univariate and multivariate analysis of the STRIPAK signature and clinical factors against overall survival (Cox Regression)

Factors tested		Univariate		Multivariate	
		HR (95%CI)	P value	HR (95%CI)	P value
STRN/STRIPAK signature		1.203 (1.095-1.322)	<0.001	1.284 (1.127-1.463)	<0.001
Clinical factors	NPI	2.874 (1.579-5.230)	0.001	2.582 (0.654-10.198)	0.176
	Grade	1.121 (0.821-1.530)	0.472	1.503 (0.756-2.985)	0.245
	Staging	1.269 (0.897-1.796)	0.178	1.331 (0.800-2.215)	0.271
	Nodal status	4.688 (1.575-14.557)	0.006	0.602 (0.060-6.006)	0.666
	ER	2.375 (0.818-6.896)	0.112	2.647 (0.785-8.930)	0.117
	Her2	3.181 (1.010-10.022)	0.048	4.682 (1.274-17.208)	0.020
Receptor subtypes	TNBC	2.417 (0.858-6.810)	0.095	0.383 (0.042-3.513)	0.396
	ER(+)/Her2(-)	2.631 (0.981-7.059)	0.055	2.119 (0.274-16.358)	0.472
	ER(-)/Her2(+)	2.871 (1.110-7.247)	0.030	4.537 (0.592-34.756)	0.145
	ER(+)/Her2(+)	2.123 (1.202-3.749)	0.010	1.435 (0.474-4.346)	0.522

3.5. STRNs and STRIPAK and patients response to drug treatment, using the TCGA/ROC plot dataset

To understand if and how STRNs and other STRIPAK partner may influence patients' response to chemotherapies, we explore the TCGA dataset that had information on tumour's pathological response and patient's response evaluated by the 5-year relapse free survival. When assessed for the pathological responses (Table-4a), it was shown that when STRN3, CCM3, MOB4A, PPP2CA and PPP2CB levels were high, patients were significantly responsive to chemotherapies. Instead, high levels of STRN4, PPP2R1A and MST1 expression are associated with a significant increase in the chance of drug resistance. In almost the same pattern when assessed for the 5-year RFS response as shown in Table-4b, patients with tumours that express high levels of STRN3, STRIP2, PPP2CA and PPP2CB were more sensitive to chemotherapies. In contrast, those with high levels of SIKE1, MOB4 and MST1 were more resisted to chemotherapies.

STRN3 is the key scaffold protein for the STRIPAK complex, of which other partner proteins dock on the duplex protein structure formed by STRN3. To assess if expression of STRN3 itself has an impact on drug responses, we further explored the link between STRN3 in the subtype of breast cancer by considering the hormone receptor status, again by the pathological and 5-year RFS response (Table-5). In ER-positive tumours and Her2-negative tumours, high STRN3 levels are significantly sensitive to chemotherapies both in the pathological and 5-years RFS responses. This is very well reflected in patients with ER(+)/Her2(-) tumours in that high STRN3 levels responded to the treatment and with ER(+)/HER2(+) tumours in the pathological responses. In contrast, high levels of STRN3 in Her2 positive tumours and Her2(+)/ER (-) subtype are associated with higher resistance to chemotherapies.

Table-4a. Patient's DRUG response, tumour pathological responses to chemotherapies*.

Molecule	Response status	Number	Transcript expression level		ROS	
			Median (Min-Max)	P value	AUC	P value
STRN3	Responders	532	428 (4-2480)	0.00002	0.565	0.000015
	Non-Responders	1100	342 (6-3394)			
STRN4	Responders	532	191 (9-1068)	1e-17	0.631	0e+00
	Non-Responders	1100	314 (6-1460)			
STRIP1 (FAM40A)	Responders	119	464 (105-1057)	0.34	0.529	0.18
	Non-Responders	388	436 (50-1339)			
STRIP2 (FAM40B)	Responders	119	54 (2-819)	0.30	0.531	0.15
	Non-Responders	388	47 (0-855)			
Calmodulin	Responders	532	1696 (52-7615)	0.15	0.522	0.076
	Non-Responders	1100	1547 (23-10294)			
SIKE1	Responders	119	452 (24-1382)	0.17	0.542	0.073
	Non-Responders	388	504 (5-4356)			
MINK1	Responders	532	1062 (285-9626)	0.53	0.51	0.26
	Non-Responders	1100	1098 (72-14670)			
CCM3 (PDCD10)	Responders	532	3443 (7-13811)	8.6e-09	0.588	3.5e-09
	Non-Responders	1100	2876 (15-13752)			
MOB4B (MOBKL1B)	Responders	532	1287 (48-5356)	0.85	0.503	0.42
	Non-Responders	1100	1270 (21-6644)			
MOB4A (MOBKL1A)	Responders	119	1255 (163-3290)	0.06	0.557	0.031
	Non-Responders	388	1097 (70-5515)			
PPP2R1A	Responders	532	538 (25-3238)	5.8e-15	0.619	3.4e-15
	Non-Responders	1100	1150 (35-4831)			
PPP2CA	Responders	532	2268 (241-5931)	0.016	0.537	0.0076
	Non-Responders	1100	2031 (87-6764)			
PPP2CB	Responders	532	2990 (195-10822)	0.00013	0.558	0.000078
	Non-Responders	1100	1510 (25-12568)			
MST1R	Responders	532	265 (10-1611)	4.1e-11	0.601	4.4e-12
	Non-Responders	1100	342 (19-1774)			
PPP2R4	Responders	532	659 (150-3102)	2.2e-21	0.645	<0.0000indef
	Non-Responders	1100	904 (99-5432)			
Caveolin	Responders	532	1542 (12-24193)	27.4e-7	0.575	3.5e-7
	Non-Responders	1100	974 (3-22206)			
TNKS2	Responders	532	866 (3-4463)	21.3e-17	0.630	<0.0000indef
	Non-Responders	1100	532 (9-2929)			

* from ROCplot.com (45).

Table-4b. Patient's DRUG response, 5-year RFS response to chemotherapies*

Molecule	Response status	n=	Transcript expression level		ROC	
			Median (Min-Max)	P value	AUC	P value
STRN3	Responders	256	451 (15-2923)	0.00099	0.587	0.00039
	Non-Responders	220	362 (32-2391)			
STRN4	Responders	256	424(107-1411)	0.42	0.521	0.21
	Non-Responders	220	393 (101-1785)			
STRIP1 (FAM40A)	Responders	115	444 (141-806)	0.78	0.514	0.39
	Non-Responders	48	411 (243-744)			
STRIP2 (FAM40B)	Responders	115	46 (1-1234)	0.074	0.589	0.042
	Non-Responders	48	34 (2-180)			
Calmodulin	Responders	256	1759 (488-6555)	0.2	0.534	0.097
	Non-Responders	220	1660 (463-5411)			
SIKE1	Responders	115	393 (5-1225)	0.0033	0.646	0.0011
	Non-Responders	48	500 (38-1027)			
MINK1	Responders	256	1169 (267-5696)	0.30	0.528	0.15
	Non-Responders	220	1266 (312-3739)			
CCM3 (PDCD10)	Responders	256	2982 (428-12107)	0.73	0.509	0.37
	Non-Responders	220	2990 (570-11370)			
MOB4B (MOBKL1B)	Responders	532	1160 (347-3723)	0.091	0.545	0.044
	Non-Responders	256	1268 (431-3500)			
MOB4A (MOBKL1A)	Responders	220	596 (116-3018)	0.81	0.512	0.40
	Non-Responders	48	563 (248-1404)			
PPP2R1A	Responders	256	1370 (348-3557)	0.80	0.507	0.40
	Non-Responders	220	1334 (420-3058)			
PPP2CA	Responders	256	2394 (665-5597)	0.00021	0.598	0.000085
	Non-Responders	220	1994 (241-5705)			
PPP2CB	Responders	256	3030 (339-11837)	0.0026	0.579	0.0013
	Non-Responders	220	2577 (785-10412)			
MST1R	Responders	256	360 (16-2343)	0.014	0.565	0.0066
	Non-Responders	220	418 (25-1351)			
PPP2R4	Responders	256	1106 (299-3980)	0.09	0.545	0.044
	Non-Responders	220	1018 (317-3727)			
Caveolin	Responders	256	1097 (15-8858)	0.21	0.533	0.11
	Non-Responders	220	16 (12599)			
TNKS2	Responders	256	798 (65-2913)	0.0068	0.572	0.0032
	Non-Responders	220	640 (114-2098))			

* from ROCplot.com (45).

Table-5. STRN3 transcript expression level and patients' response to chemotherapies in subtypes of breast cancer (* by Mann-Whitney U test)#

Hormone receptor and subtypes		Pathological response			5-year RFS response				
		Response status	Number	Median (Min-Max)	P value	Response status	Number	Median (Min-Max)	P value
ER status	ER (-)	Responders	279	338 (15-2480)	0.70	Responders	115	446 (15-2014)	0.12
		Non-Responders	387	351 (32-3394)		Non-Responders	111	360 (32-2391)	
	ER (+)	Responders	253	517 (4-1927)	1.4e-10	Responders	141	454 (16-2923)	0.0025
		Non-Responders	713	338 (6-3160)		Non-Responders	109	363 (85-1092)	
Her2 status	Her2 (-)	Responders	389	505 (4-2480)	6.2e-12	Responders	183	409 (15-1610)	0.0043
		Non-Responders	890	336 (6-3160)		Non-Responders	173	331 (32-1104)	
	Her2 (+)	Responders	143	301 (64-2190)	0.0014	Responders	73	593 (133-2923)	0.31
		Non-Responders	210	404 (18-3394)		Non-Responders	47	549 (153-2391)	
ER/Her2 status subtypes	ER(-)/Her2(+)	Responders	83	304 (64-2190)	0.0034	Responders	35	655 (133-2014)	0.69
		Non-Responders	110	419 (106-3394)		Non-Responders	26	580 (161-2391)	
	ER(+)/Her2(-)	Responders	193	720 (4-1927)	2.3e-16	Responders	103	409 (16-1349)	0.017
		Non-Responders	613	334 (6-3160)		Non-Responders	88	336 (85-1092)	
	ER(+)/Her2(+)	Responders	60	288 (76-1564)	0.053	Responders	38	579 (216-2923)	0.1
		Non-Responders	100	364 (18-2645)		Non-Responders	21	512 (153-957)	
	TNBC	Responders	196	428 (15-2480)	0.14	Responders	80	413 (15-1610)	0.13
		Non-Responders	277	339 (32-2180)		Non-Responders	84	328 (32-1104)	

* from ROCplot.com (45).

3.6. Creation of STRN knockdown and STRN3 knockdown models from breast cancer cell lines with different receptor status

In the light of the findings that STRIPAK complex molecules had a significant bearing on the clinical progression and in particular on the clinical outcome of the patients, as well as patient's response to drug treatment, we created a set of breast cancer cell models to further investigate this link. We have chosen 4 breast cancer cell lines, each representing a subtype of breast cancer with different hormone receptor status. They were ER(+)/Her2(-) MCF7, ER(-)/Her2(+) SKBR3, ER(-)/Her2(-) MDAMB-231 and ER(+)/Her2(+) MDA MB-361. The knockdown efficiency of STRN and STRN3 are illustrated in Figure 4 (upper panel). We had also tested the protein expression profile of the two molecules before and after knockdown in the breast cancer cell lines by Western blot (Figure 4 lower panel). The cell models created were subsequently use for *in vitro* experiments.

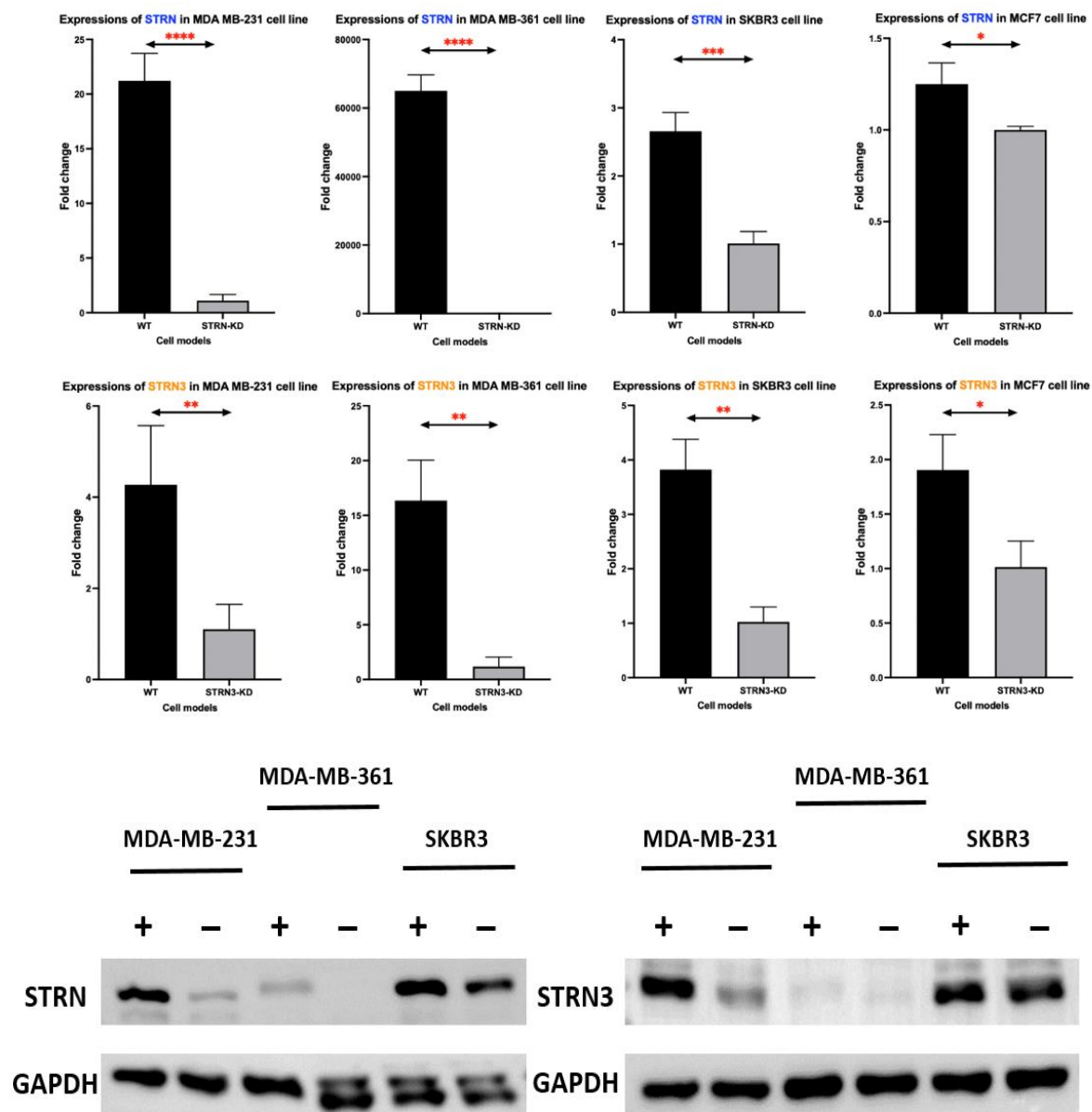
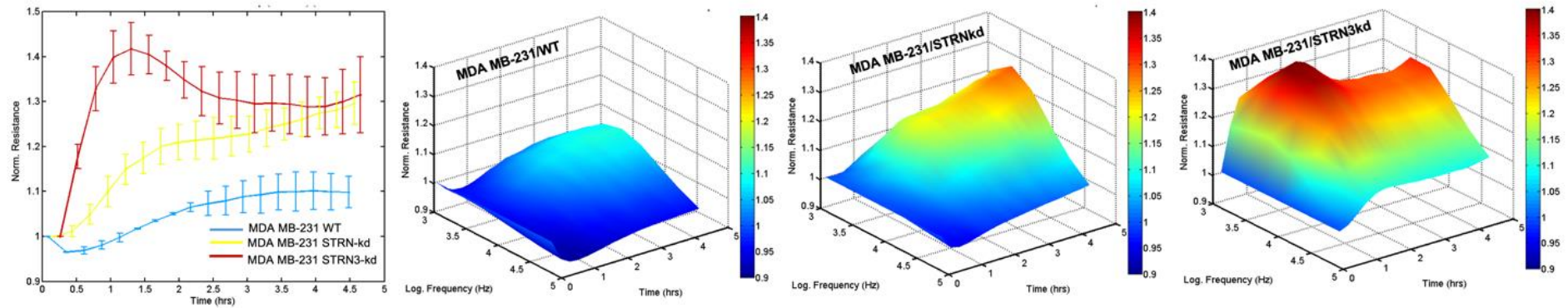


Figure-2. Top panel: qPCR confirmation of knockdowns- Semiquantitative analysis of the relative gene expression of STRN and STRN3 in the four breast cancer cell lines, MDA MB-231, MDA MD-361, SKBR3, MCF7. The fold change was acquired by $2^{-\Delta\Delta C_t}$ which is a formula used to calculate the relative fold change expression when performing real-time PCR. Unpaired t-test was performed to statistically analysing the knockdowns with * = $P < 0.05$, ** = $P < 0.01$, *** = $P < 0.001$, **** = $P < 0.0001$. Bottom panel: Western blot shows the STRN and STRN3's protein expression respectively in the WT (+) and the KD (-) MDA-MB-231, MDA-MB361 and SKBR3 cell lines. The corresponded protein expression of the housekeeping gene, GAPDH, in each cell model is also demonstrated.

MDA MB-231 Adhesion assay



MDA MB-231 Wounding assay

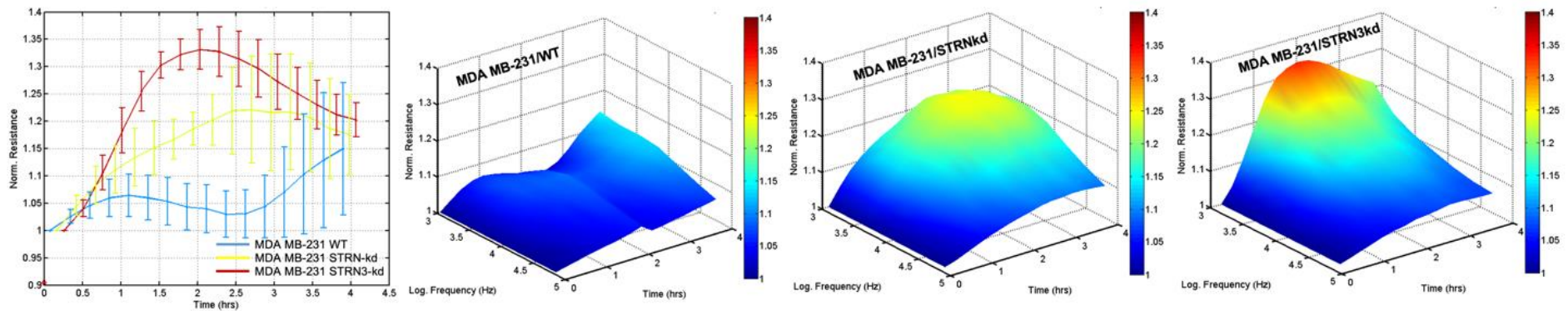
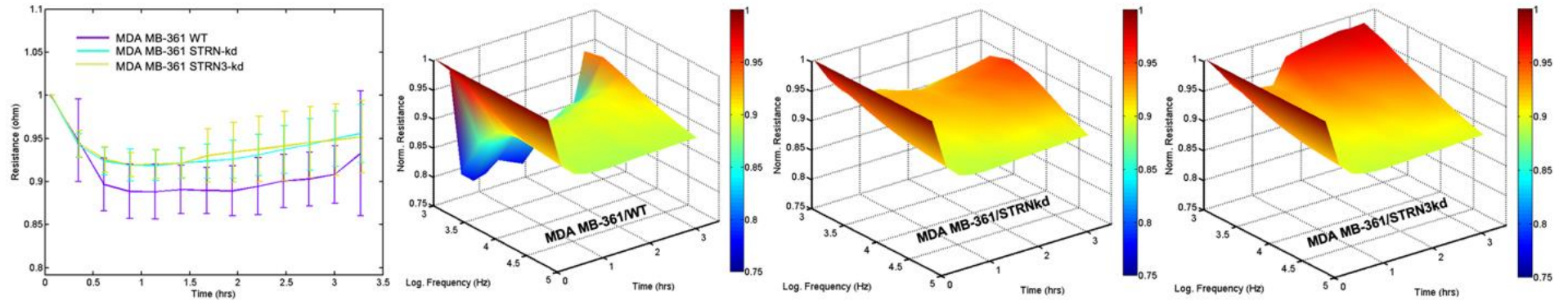


Figure 3A. Cell adhesiveness and migration of MDA MB-231 cells with different STRNs expressions, namely MDA MB-231 WT, MDA MB-231 STRNkd and MDA MB-231 STRN3kd. Top panel: adhesion assay; Bottom panel: migration assay. From left to right, first lane: 2D graph compare the cell responses among the cell models detected at 4000Hz (resistance with SD); second lane: 3D graph of cell responses for WT cells; third lane: 3D graph of cell responses for STRNkd cells; fourth lane: 3D graph of cell responses STRN3kd cells. The 3D figures indicate cells responses (Z-axis, normalized resistance in ohms) over time (X-axis, hours) and across multiple frequencies (Y-axis, Hz). All resistance detected were normalized with the initial result acquired.

MDA MB-361 Adhesion assay



MDA MB-361 Wounding assay

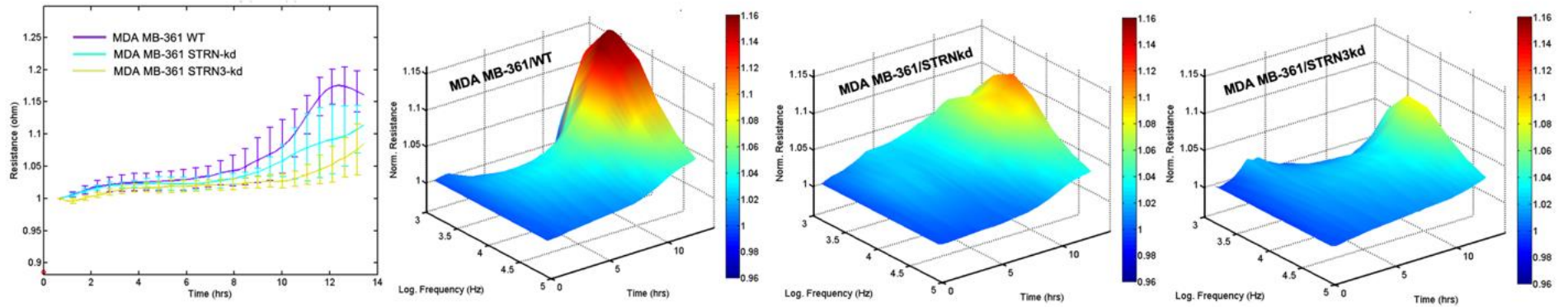
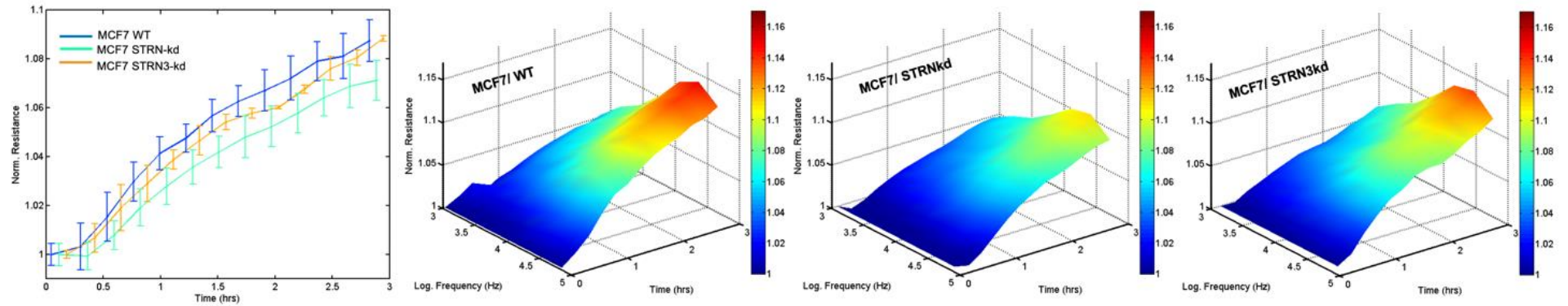


Figure 3B. Cell adhesiveness and migration of MDA MB-361 cells with different STRNs expressions, namely MDA MB-361 WT, MDA MB-361 STRNkd and MDA MB-361 STRN3kd. Top panel: adhesion assay; Bottom panel: migration assay. From left to right, first lane: 2D graph compare the cell responses among the cell models detected at 4000Hz (resistance with SD); second lane: 3D graph of cell responses for WT cells; third lane: 3D graph of cell responses for STRNkd cells; fourth lane: 3D graph of cell responses for STRN3kd cells. The 3D figures indicate cells responses (Z-axis, normalized resistance in ohms) over time (X-axis, hours) and across multiple frequencies (Y-axis, Hz). All resistance detected were normalized with the initial result acquired.

MCF7 Adhesion assay



MCF7 Wounding assay

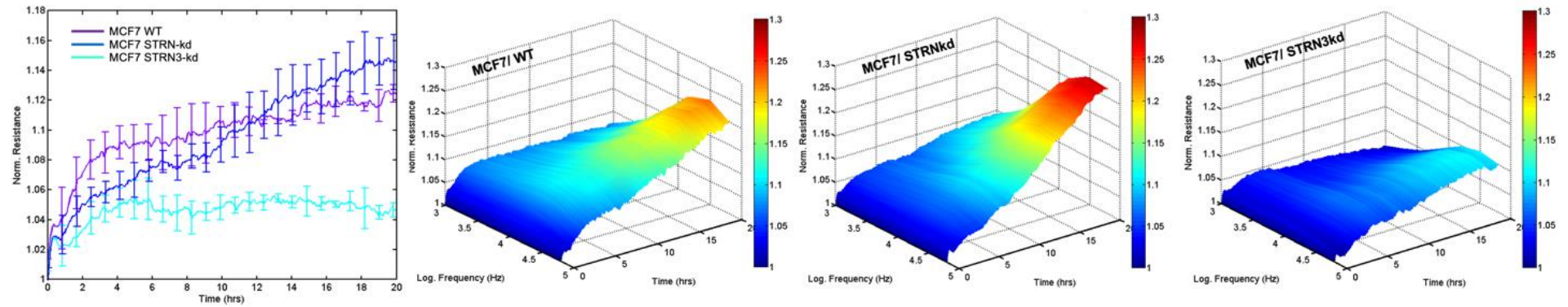
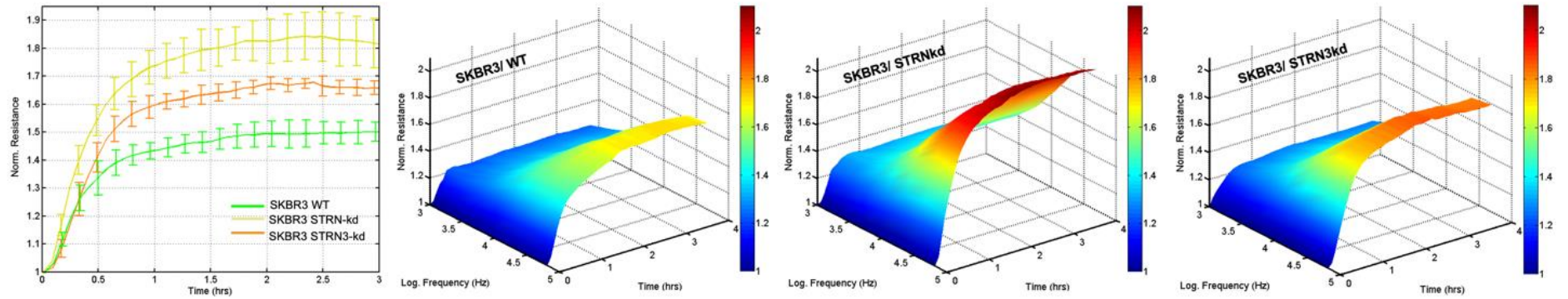


Figure 3C. Cell adhesiveness and migration of MCF7 cells with different STRNs expressions, namely MCF7 WT, MCF7 STRNkd and MCF7 STRN3kd. Top panel: adhesion assay; Bottom panel: migration assay. From left to right, first lane: 2D graph compare the cell responses among the cell models detected at 4000Hz (resistance with SD); second lane: 3D graph of cell responses for WT cells; third lane: 3D graph of cell responses for STRNkd cells; fourth lane: 3D graph of cell responses for STRN3kd cells. The 3D figures indicate cells responses (Z-axis, normalized resistance in ohms) over time (X-axis, hours) and across multiple frequencies (Y-axis, Hz). All resistance detected were normalized with the initial result acquired.

SKBR3 Adhesion assay



SKBR3 Wounding assay

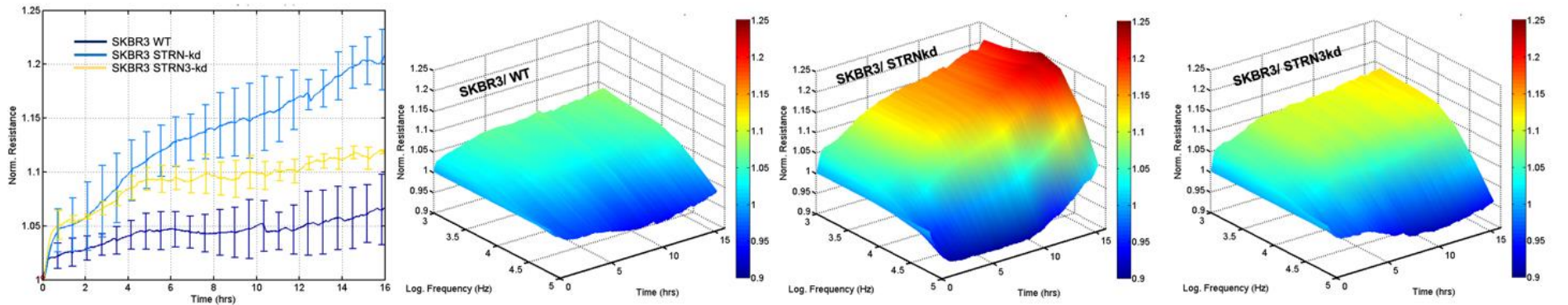


Figure 3D. Cell adhesiveness and migration of SKBR3 cells with different STRNs expressions, namely SKBR3 WT, SKBR3 STRNkd and SKBR3 STRN3kd. Top panel: adhesion assay; Bottom panel: migration assay. From left to right, first lane: 2D graph compare the cell responses among the cell models detected at 4000Hz (resistance with SD); second lane: 3D graph of cell responses for WT cells; third lane: 3D graph of cell responses for STRNkd cells; fourth lane: 3D graph of cell responses for STRN3kd cells. The 3D figures indicate cells responses (Z-axis, normalized resistance in ohms) over time (X-axis, hours) and across multiple frequencies (Y-axis, Hz). All resistance detected were normalized with the initial result acquired.

3.7 The effects of STRN and STRN3 knock down on cell behaviour in breast cancer cells with different receptor status

All the four cell lines were chosen for ECIS application. By varying the frequency of the applied current, ECIS could distinguish intercellular resistance and cell to matrix resistance. The resistance measured at lower frequency could provide more accurate data regarding the dynamic change of cell-cell contact, as low frequency current is more likely to go under and between the cell gaps. The firmer the cell junction, the greater the resistance at lower frequency. In contrast, higher frequency current is more optimal for measuring cell-matrix interactions and thereby the cell attachment. While more cells adhere to the 96-well plate base along with time, the resistance increases. Meanwhile, the rate of cell adhesion could be reflected by the steepness of the line.

In this study, the attachment and spreading of these cells with and without STRN or STRN3 knock-down were real-time monitored. As we can see from Figure 3A which represented the cell behaviour changes of MDA-MB-231 cells, the WT cells had the lowest resistance throughout both adhesion and wound healing period compared with the other two MDA-MB-231 KD cell models. The same pattern across all frequencies was seen in the corresponded 3D graphs (Figure 3A). The lower the frequency, the higher resistance for the two KD cell lines and the differences with the WT cell. The results indicated the reduced expression of STRNs, especially STRN3, would facilitate cell adhesion and migration in triple negative breast cancer cells.

MDA-MD-361 with and without STRNs KD responded in an opposite way during cell attachment and wound healing compared with MDA-MB231 (Figure 3B). The behaviour differences between STRNkd and STRN3kd cells were not obvious at 4000Hz, yet they both displayed greater cell-matrix adhesiveness while had reduced spreading during wounding process when compared with the WT cells. The reduced migration after STRNs member KD was also seen in MCF7 cells, another ER positive cell line, of which the resistance during wound healing was greatly suppressed especially with STRN3 KD (Figure 3C). Similar trend was also observed during the attachment process in a less striking way that the MCF WT cells exhibited stronger adhesiveness, although the difference was not highly significant (Figure 3C).

In opposite to what we have observed in ER(+)/HER2(-) cell, SKBR3 with opposite receptor status exhibited contrasted cell response during adhesion and migration (Figure 3D). As an ER(-)/Her2(+) cell line, STRN and STRN3 significantly facilitated both processes with STRN3 contributed more to attachment and STRN in cell motility. Moreover, the cell-matrix and cell-cell interactions were higher in the STRNs KD groups during adhesion and migration, respectively, as can be indicated from the 3D graphs, which reflected resistance at different frequencies.

We have additionally validated the finding from the automated ECIS analyses on the cell models by employing a traditional cell-matrix adhesion assay. As shown in Figure 3, the MDA-MB-231 STRNkd and STRN3kd cells showed significantly increased number of adhered cells at the time of fixation compared with the control MDA MB 231 WT cells. This result has aligned with our finding reflected from ECIS application. Similar trend but to less degree has observed in MDA-MB-361, with the KD cells exhibited greater adhesion ability to the gel base (Figure-4).

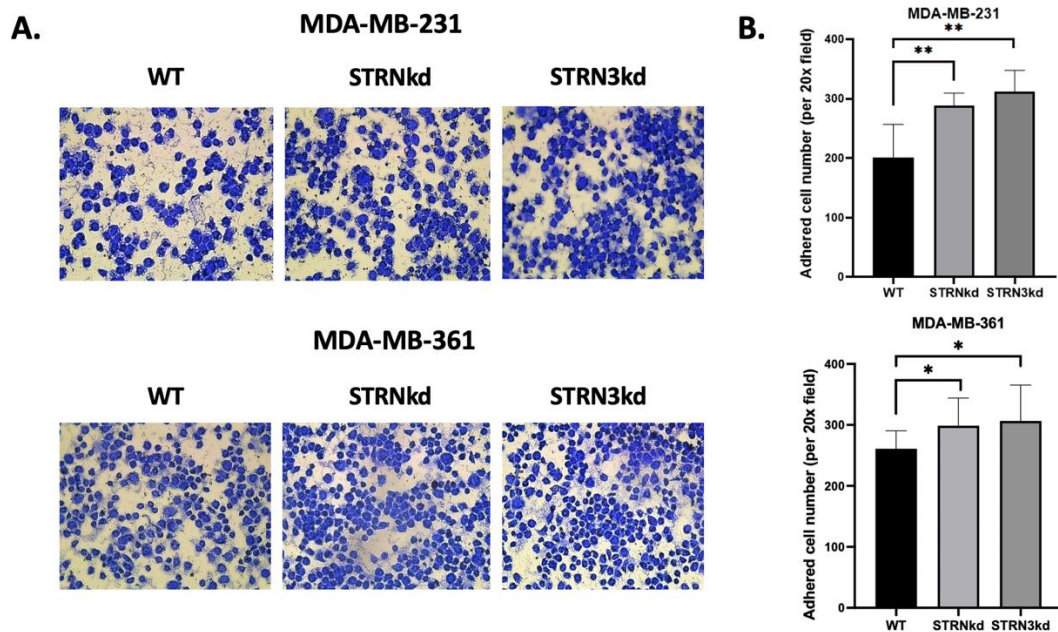


Figure 4. Matrigel adhesion assay of MDA-MB-231 (up) and MDA-MB-361 (bottom). (A) Representative images of the adhered cells captured at 20X magnification. (B) Bar graphs of the adhered cell number for each cell model (n=12). *p<0.05; **p<0.01 for comparisons between the KD and the WT cells.

Table-6. IC50 of chemo-drugs tests

	MDA MB-231/WT	MDA MB-231/STRNkd	MDA MB-231/STRN3kd
Paclitaxel	58.6nM	167nM	279nM
Docetaxel	24.3nM	31.9nM	32,2nM
	MDA MB-361/WT	MDA MB-361/STRNkd	MDA MB-361/STRN3kd
Paclitaxel	14nM	19nM	14.2nM
Docetaxel	5.23nM	0.8nM	5.29nM
	MCF7/WT	MCF7/STRNkd	MCF7/STRN3kd
Paclitaxel	4.74nM	0.726nM	2.69nM
Docetaxel	0.95nM	0.55nM	6.5nM
	SKBR3/WT	SKBR3/STRNkd	SKBR3/STRN3kd
Paclitaxel	7.34nM	0.12nM	9.03nM
Docetaxel	4.9nM	13.63nM	0.39nM

3.9 Expression of STRNs in breast cancer cell response to chemodrugs, determined by in vitro study.

The four breast cancer cell lines were subsequently tested with their responses to chemotherapy drugs following confirmation of knockdown of STRN and STRN3 (Table-6). Under the used in vitro condition, MDA MB-231 (triple negative) cells that had reduced expression of STRNs family members, especially STRN3 had higher IC50 to both chemodrugs, revealing an increase in drug resistance after knock downing STRN or STRN3 compared with WT cells. No difference in drug resistance was observed between the WT MDA MB-361 and the corresponded STRN3kd cells, while the cells with STRNkd were being more responsive to docetaxel. Whilst the lack in expression of STRN3 suppressed the MCF7 cells' sensitivity to docetaxel, it induced lower IC50 in SKBR3 cells with STRN3kd, elevating the toxicity of docetaxel to SKBR3 STRN3kd cells. In terms of the drug responses

of MCF7 and SKBR3 to paclitaxel, the cells that were less in STRN level had shown better response to the drug therapy compared with the respective WT and STRN3kd cells.

4. Discussion

In this report, we have shown for the first time the full profile of STRNs and their binding-partner proteins in STRIPAK complex, as well as their relationships to breast cancer patients' responses to drug treatment and clinical outcomes. The study also examined the impact of targeting of the backbone of the STRIPAK, namely STRNs, in cell models on cell behaviour and cell's responsiveness to chemo-drugs together with the information on clinical drug responses in relationship with STRNs and the STRIPAK partners.

The STRIPAK complex, with STRNs act as center, contains both kinases and phosphatases. STRIPAKs play critical roles in processes of protein phosphorylation and dephosphorylation, serving as important regulators of multiple signaling pathways involved in cell growth, differentiation, proliferation, and apoptosis. Growing evidence support the connection of dysregulation of STRIPAK complexes to cancer and other human diseases.

Protein phosphatase 2A (PP2A) is a heterotrimeric Ser/Thr phosphatase that regulates numerous cellular processes. It has been shown that PP2A is dysregulated in several human diseases, including cancer. An essential role of PP2A for controlling cell growth, cancer development and thereby act as a tumour suppressor has also been studied.

In the current study, we have made several major findings. First, we observed that high expressions of STRN3, STRN4 and CALM were associated with shorter overall survival (OS) of the patients and combination of these three molecules resulted in an excellent indicator of poor prognosis. Our finding is consistent with previous publications on overexpression of STRN3, STRN4 and CALM in some cancers. For example, in gastric cancer (GC) tissues and cell lines, CALM2 expression was elevated and positively relevant to the poor prognosis of GC patients; *in vivo* experiments also confirmed that CALM2 boosted tumour growth and lung metastasis [46].

Secondly, we observed that higher levels of PPP2A, PPP2B and PPPR1A in patients with significantly longer OS; combination of these three biomarkers leads to a favourable prognostic indicator. This finding is also consistent with the previous reports on PPP2A behaving as a tumor suppressor. We have also found that integration of both STRNs group and PPP2 protein family members constitutes a highly significant prognostic indicator for both OS and DFS, which is independent of other factors (clinical, pathological, or receptor status). It was also interesting that the new biomarker signature, when combined with traditional markers including ER and Her2 can further identify subgroup of patients who had worst performance, namely those with ER negative, Her-2 positive and ER-negative/Her2-positive subtypes, affording additional value to this finding. This would need further validation in a much enlarged cohort of patients in the future.

Our *in vitro* study on cells' behaviour has suggested that the expression of STRN and STRN3 could influence the cell-cell interaction during both cell adhesion and migration periods. According to a recent study which proposed a contribution of STRN in both adherent junction and tight junctions [6], further *in vitro* studies might be conducted to assess the integrity and barrier functions of epithelial cells in various epithelial tissues after STRNs knockdown.

By analysis of the clinical results, we also observed that higher STRN3 expression was strongly associated with better tumour pathological responses to chemotherapy in patients who exhibited ER (+)/ HER2(-) status, in contrast to ER (-)/ HER2(+) patients with high expression of STRN3 who have shown greater resistance to chemo-drugs. This observation was aligned with our in-vitro chemo-drug test of MCF7 (ER (+)/ HER2(-)) and SKBR3 (ER (-)/ HER2(+)) cells' responses to one of the chemo-drug tested, namely Docetaxel. Interestingly, no difference in IC50 values was observed between WT MDA MB-361 (ER (+)/ HER2(+)) and the STRN3kd cells when they were treated with Docetaxel or Paclitaxel. Whilst our clinical results indicated patients with ER (+)/ HER2(+) showed better response to chemotherapies when they have decreased STRN3 expression, we also found that higher expression of STRN3 was associated with increased drug sensitivity in patients exhibited HER2(+) (Table 6). The combined impact of the receptor status in response to chemotherapies might thereby

explain our results. Thus, the present study has provided some important information on the link between the STRIPAK and STRNs in evaluating patient's clinical response to drug therapies.

However, the present study has its limit. The expression analysis has been conducted on a historical collection of fresh frozen tissues. The present study has an advantage in that the tested molecules were free from the influence of drug intervention as none of the patients received neoadjuvant therapy prior to surgery. It would be, however, ideal to validate the study on an independent cohort, similarly unaffected by the pre-surgery treatment. This option was not available to the present study, and we hope in future, carefully selected datasets from a public database would be able to help address this limit. Additionally, it is essential to investigate the mechanistic role of STRIPAK in chemo-resistance at protein levels, by looking into the signaling events that the STRIPAK complex involved, such as the Hippo signal pathway. It has been shown that the Hippo-STRIPAK complex plays an essential role in regulating DNA double-stranded break repair and genomic stability [17]. Thus, a future project would be to examine the possible contribution of the STRIPAK signature and mutations of the gene related to these pathways including the HRR (homologous recombination repair) genes and the homologous recombination deficiency genes (HRD) to patients response to drug such as the PARP inhibitors. STE20-like protein kinases 1 and 2 (MST1/2) has also been reported to directly phosphorylate the zinc finger MYND type-containing 8 or ZMYND8, leading to the suppression of DNA repair in the nucleus. However, MST1/2 inactivation by STRIPAK could increase the DNA repair capacity and contribute to chemoresistance in cancer cells. In contrast, STRIPAK inhibitors could recover the kinase activity of MST1/2, resulting in re-sensitization of cancer cells to chemotherapy. Since STRN3 function as a cornerstone of the STRIPAK complex, finding a potential therapeutic inhibitor to STRN3 and thereby disrupting the whole complex structure could also be our next step investigation. Future studies should focus on investigating the exact roles of the STRIPAK complex in cancer development and progression.

Funding: The study was supported by the Cardiff University China Medical Scholarship.

Acknowledgements: The authors wish to acknowledge Cardiff University China Medical Scholarship.

Author Contributions: Conceptualization, W.G.J; Formal analysis, A.X.L., J.Z., F.R. and W.G.J ; Investigation, A.X.L., J.Z., F.R., A.S., W.G.J; Methodology, F.R., A.X.L., E.K., Q.P.D.; W.G.J; Resources, W.G.J., E.D; Supervision, W.G.J., T.A.M; Validation, W.G.J., F.R., A.X.L; Writing – original draft, A.X.L., W.G.J., Q.P.D; Writing – review & editing, W.G.J., Q.P.D., L.Y., E.L.

Institutional Review Board Statement: The study was approved by the local ethics committee.

Informed Consent Statement: Informed consent was obtained from all subjects in the study.

Conflict of Interest: The authors declare no conflict of interest.

References

1. Muro Y, Chan EK, Landberg G, Tan EM: A cell-cycle nuclear autoantigen containing WD-40 motifs expressed mainly in S and G2 phase cells. *Biochem Biophys Res Commun* 1995, 207(3):1029-1037.
2. Castets F, Bartoli M, Barnier JV, Baillat G, Salin P, Moqrich A, Bourgeois JP, Denizot F, Rougon G, Calothy G *et al*: A novel calmodulin-binding protein, belonging to the WD-repeat family, is localized in dendrites of a subset of CNS neurons. *J Cell Biol* 1996, 134(4):1051-1062.
3. Castets F, Rakitina T, Gaillard S, Moqrich A, Mattei MG, Monneron A: Zinedin, SG2NA, and striatin are calmodulin-binding, WD repeat proteins principally expressed in the brain. *J Biol Chem* 2000, 275(26):19970-19977.
4. Gaillard S, Bartoli M, Castets F, Monneron A: Striatin, a calmodulin-dependent scaffolding protein, directly binds caveolin-1. *FEBS Lett* 2001, 508(1):49-52.
5. Nader M, Alotaibi S, Alsolme E, Khalil B, Abu-Zaid A, Alsomali R, Bakheet D, Dzimiri N: Cardiac striatin interacts with caveolin-3 and calmodulin in a calcium sensitive manner and regulates cardiomyocyte spontaneous contraction rate. *Can J Physiol Pharmacol* 2017, 95(10):1306-1312.
6. Lahav-Ariel L, Caspi M, Nadar-Ponniah PT, Zelikson N, Hofmann I, Hanson KK, Franke WW, Sklan EH, Avraham KB, Rosin-Arbesfeld R: Striatin is a novel modulator of cell adhesion. *FASEB J* 2019, 33(4):4729-4740.
7. Moqrich A, Mattei MG, Bartoli M, Rakitina T, Baillat G, Monneron A, Castets F: Cloning of human striatin cDNA (STRN), gene mapping to 2p22-p21, and preferential expression in brain. *Genomics* 1998, 51(1):136-139.
8. Goudreault M, D'Ambrosio LM, Kean MJ, Mullin MJ, Larsen BG, Sanchez A, Chaudhry S, Chen GI, Sicheri F, Nesvizhskii AI *et al*: A PP2A phosphatase high density interaction network identifies a novel striatin-interacting phosphatase and kinase complex linked to the cerebral cavernous malformation 3 (CCM3) protein. *Mol Cell Proteomics* 2009, 8(1):157-171.
9. Hwang J, Pallas DC: STRIPAK complexes: structure, biological function, and involvement in human diseases. *Int J Biochem Cell Biol* 2014, 47:118-148.
10. Kean MJ, Ceccarelli DF, Goudreault M, Sanches M, Tate S, Larsen B, Gibson LC, Derry WB, Scott IC, Pelletier L *et al*: Structure-function analysis of core STRIPAK Proteins: a signaling complex implicated in Golgi polarization. *J Biol Chem* 2011, 286(28):25065-25075.
11. Kuck U, Radchenko D, Teichert I: STRIPAK, a highly conserved signaling complex, controls multiple eukaryotic cellular and developmental processes and is linked with human diseases. *Biol Chem* 2019, 400(8):1005-1022.
12. Hyodo T, Ito S, Hasegawa H, Asano E, Maeda M, Urano T, Takahashi M, Hamaguchi M, Senga T: Misshapen-like kinase 1 (MINK1) is a novel component of striatin-interacting phosphatase and kinase (STRIPAK) and is required for the completion of cytokinesis. *J Biol Chem* 2012, 287(30):25019-25029.
13. Gordon J, Hwang J, Carrier KJ, Jones CA, Kern QL, Moreno CS, Karas RH, Pallas DC: Protein phosphatase 2a (PP2A) binds within the oligomerization domain of striatin and regulates the phosphorylation and activation of the mammalian Ste20-Like kinase Mst3. *BMC Biochem* 2011, 12:54.
14. Nordzieke S, Zobel T, Franzel B, Wolters DA, Kuck U, Teichert I: A fungal sarcolemmal membrane-associated protein (SLMAP) homolog plays a fundamental role in development and localizes to the nuclear envelope, endoplasmic reticulum, and mitochondria. *Eukaryot Cell* 2015, 14(4):345-358.
15. Schad EG, Petersen CP: STRIPAK Limits Stem Cell Differentiation of a WNT Signaling Center to Control Planarian Axis Scaling. *Curr Biol* 2020, 30(2):254-263 e252.
16. Lu J, Hu Z, Deng Y, Wu Q, Wu M, Song H: MEKK2 and MEKK3 orchestrate multiple signals to regulate Hippo pathway. *J Biol Chem* 2021, 296:100400.
17. An L, Cao Z, Nie P, Zhang H, Tong Z, Chen F, Tang Y, Han Y, Wang W, Zhao Z *et al*: Combinatorial targeting of Hippo-STRIPAK and PARP elicits synthetic lethality in gastrointestinal cancers. *J Clin Invest* 2022, 132(9).
18. Breitman M, Zilberberg A, Caspi M, Rosin-Arbesfeld R: The armadillo repeat domain of the APC tumor suppressor protein interacts with Striatin family members. *Biochim Biophys Acta* 2008, 1783(10):1792-1802.
19. Franke WW, Rickelt S, Zimbelmann R, Dorflinger Y, Kuhn C, Frey N, Heid H, Rosin-Arbesfeld R: Striatins as plaque molecules of zonulae adherentes in simple epithelia, of tessellate junctions in stratified epithelia, of cardiac composite junctions and of various size classes of lateral adherens junctions in cultures of epithelia- and carcinoma-derived cells. *Cell Tissue Res* 2015, 359(3):779-797.
20. Zheng S, Sun P, Liu H, Li R, Long L, Xu Y, Chen S, Xu J: 17beta-estradiol upregulates striatin protein levels via Akt pathway in human umbilical vein endothelial cells. *PLoS One* 2018, 13(8):e0202500.
21. Belachew EB, Sewasew DT: Molecular Mechanisms of Endocrine Resistance in Estrogen-Positive Breast Cancer. *Front Endocrinol (Lausanne)* 2021, 12:599586.
22. Xie R, Wen F, Qin Y: The Dysregulation and Prognostic Analysis of STRIPAK Complex Across Cancers. *Front Cell Dev Biol* 2020, 8:625.
23. Zhang Y, Gu X, Jiang F, Sun P, Li X: Altered expression of striatin-4 is associated with poor prognosis in bladder transitional cell carcinoma. *Oncol Lett* 2021, 21(4):331.
24. Czauderna C, Poplawski A, O'Rourke CJ, Castven D, Perez-Aguilar B, Becker D, Heilmann-Heimbach S, Odenthal M, Amer W, Schmiel M *et al*: Epigenetic modifications precede molecular alterations and drive human hepatocarcinogenesis. *JCI Insight* 2021, 6(17).
25. Ito M, Hiwasa T, Oshima Y, Yajima S, Suzuki T, Nanami T, Sumazaki M, Shiratori F, Funahashi K, Takizawa H *et al*: Identification of serum anti-striatin 4 antibodies as a common marker for esophageal cancer and other solid cancers. *Mol Clin Oncol* 2021, 15(5):237.
26. Wong M, Hyodo T, Asano E, Funasaka K, Miyahara R, Hirooka Y, Goto H, Hamaguchi M, Senga T: Silencing of STRN4 suppresses the malignant characteristics of cancer cells. *Cancer Sci* 2014, 105(12):1526-1532.
27. Jiang F, Zheng Q, Chang L, Li X, Wang X, Gu X: Pro-oncogene Pokemon Promotes Prostate Cancer Progression by Inducing STRN4 Expression. *J Cancer* 2019, 10(8):1833-1845.
28. Xie Y, Zhao F, Zhang P, Duan P, Shen Y: miR-29b inhibits non-small cell lung cancer progression by targeting STRN4. *Hum Cell* 2020, 33(1):220-231.

29. Qiu LM, Sun YH, Chen TT, Chen JJ, Ma HT: STRIP2, a member of the striatin-interacting phosphatase and kinase complex, is implicated in lung adenocarcinoma cell growth and migration. *FEBS Open Bio* 2020, 10(3):351-361.
30. Gupta R, Kumar G, Jain BP, Chandra S, Goswami SK: Ectopic expression of 35 kDa and knocking down of 78 kDa SG2NAs induce cytoskeletal reorganization, alter membrane sialylation, and modulate the markers of EMT. *Mol Cell Biochem* 2021, 476(2):633-648.
31. Kelly LM, Barila G, Liu P, Evdokimova VN, Trivedi S, Panebianco F, Gandhi M, Carty SE, Hodak SP, Luo J *et al*: Identification of the transforming STRN-ALK fusion as a potential therapeutic target in the aggressive forms of thyroid cancer. *Proc Natl Acad Sci U S A* 2014, 111(11):4233-4238.
32. Park G, Kim TH, Lee HO, Lim JA, Won JK, Min HS, Lee KE, Park DJ, Park YJ, Park WY: Standard immunohistochemistry efficiently screens for anaplastic lymphoma kinase rearrangements in differentiated thyroid cancer. *Endocr Relat Cancer* 2015, 22(1):55-63.
33. Kusano H, Togashi Y, Akiba J, Moriya F, Baba K, Matsuzaki N, Yuba Y, Shiraishi Y, Kanamaru H, Kuroda N *et al*: Two Cases of Renal Cell Carcinoma Harboring a Novel STRN-ALK Fusion Gene. *Am J Surg Pathol* 2016, 40(6):761-769.
34. Yang Y, Qin SK, Zhu J, Wang R, Li YM, Xie ZY, Wu Q: A Rare STRN-ALK Fusion in Lung Adenocarcinoma Identified Using Next-Generation Sequencing-Based Circulating Tumor DNA Profiling Exhibits Excellent Response to Crizotinib. *Mayo Clin Proc Innov Qual Outcomes* 2017, 1(1):111-116.
35. Su C, Jiang Y, Jiang W, Wang H, Liu S, Shao Y, Zhao W, Ning R, Yu Q: STRN-ALK Fusion in Lung Adenocarcinoma with Excellent Response Upon Alectinib Treatment: A Case Report and Literature Review. *Onco Targets Ther* 2020, 13:12515-12519.
36. Sun K, Nie L, Nong L, Cheng Y: Primary resistance to alectinib in a patient with STRN-ALK-positive non-small cell lung cancer: A case report. *Thorac Cancer* 2021, 12(12):1927-1930.
37. Furugaki K, Harada N, Yoshimura Y: Sensitivity of eight types of ALK fusion variant to alectinib in ALK-transformed cells. *Anticancer Drugs* 2022, 33(2):124-131.
38. Bisoyi P, Devi P, Besra K, Prasad A, Jain BP, Goswami SK: The profile of expression of the scaffold protein SG2NA(s) differs between cancer types and its interactome in normal vis-a-vis breast tumor tissues suggests its wide roles in regulating multiple cellular pathways. *Mol Cell Biochem* 2022, 477(6):1653-1668.
39. Lu Q, Pallas DC, Surks HK, Baur WE, Mendelsohn ME, Karas RH: Striatin assembles a membrane signaling complex necessary for rapid, nongenomic activation of endothelial NO synthase by estrogen receptor alpha. *Proc Natl Acad Sci U S A* 2004, 101(49):17126-17131.
40. Tan B, Long X, Nakshatri H, Nephew KP, Bigsby RM: Striatin-3 gamma inhibits estrogen receptor activity by recruiting a protein phosphatase. *J Mol Endocrinol* 2008, 40(5):199-210.
41. Jiang WG, Watkins G, Lane J, Cunnick GH, Douglas-Jones A, Mokbel K, Mansel RE: Prognostic value of rho GTPases and rho guanine nucleotide dissociation inhibitors in human breast cancers. *Clin Cancer Res* 2003, 9(17):6432-6440.
42. Giaeve I, Keese CR: Micromotion of mammalian cells measured electrically. *Proc Natl Acad Sci U S A* 1991, 88(17):7896-7900.
43. Yang Y, Sanders AJ, Ruge F, Dong X, Cui Y, Dou QP, Jia S, Hao C, Ji J, Jiang WG: Activated leukocyte cell adhesion molecule (ALCAM)/CD166 in pancreatic cancer, a pivotal link to clinical outcome and vascular embolism. *Am J Cancer Res* 2021, 11(12):5917-5932.
44. Frugtniet BA, Martin TA, Zhang L, Jiang WG: Neural Wiskott-Aldrich syndrome protein (nWASP) is implicated in human lung cancer invasion. *BMC Cancer* 2017, 17(1):224.
45. Fekete JT, Gyorffy B: ROCplot.org: Validating predictive biomarkers of chemotherapy/hormonal therapy/anti-HER2 therapy using transcriptomic data of 3,104 breast cancer patients. *Int J Cancer* 2019, 145(11):3140-3151.
46. Mu G, Zhu Y, Dong Z, Shi L, Deng Y, Li H: Calmodulin 2 Facilitates Angiogenesis and Metastasis of Gastric Cancer via STAT3/HIF-1A/VEGF-A Mediated Macrophage Polarization. *Front Oncol* 2021, 11:727306.

Legend to figures

Figure-1. Integrated STRN and other core STRIPK members and the prediction of patient survival. The expression pattern of the shortlist STRIPAKs are tested using ROC method (A). There is a significant predictive value in predicting the OS (AUC=0.836). Patients were then stratified into two groups based on their expression pattern of the signature. The stratification showed a highly significant value in predicting the overall survival ($p<0.0001$) (B) and disease-free survival (C). The signature identified those patients who had worst outcome in ER negative tumours (D1), Her-2 positive tumours (E2) and more profoundly in ER(-)/Her2(+) tumours (F1), whereas it had little additional value for ER(+) tumours (D2), Her-2 negative tumours (E1) and TNBC tumours (F2).

Figure-2. Top panel: qPCR confirmation of knockdowns- Semiquantitative analysis of the relative gene expression of STRN and STRN3 in the four breast cancer cell lines, MDA MB-231, MDA MD-361, SKBR3, MCF7. The fold change was acquired by $2^{-\Delta\Delta C_t}$ which is a formula used to calculate the relative fold change expression when performing real-time PCR. Unpaired t-test was performed to statistically analysing the knockdowns with *= $P<0.05$, **= $P<0.01$, ***= $P<0.001$, ****= $P<0.0001$.

Bottom panel: Western blot shows the STRN and STRN3's protein expression respectively in the WT (+) and the KD (-) MDA-MB-231, MDA-MB361 and SKBR3 cell lines. The corresponded protein expression of the housekeeping gene, GAPDH, in each cell model is also demonstrated.

Figure 3A. Cell adhesiveness and migration of MDA MB-231 cells with different STRNs expressions, namely MDA MB-231 WT, MDA MB-231 STRNkd and MDA MB-231 STRN3kd. Top panel: adhesion assay; Bottom panel: migration assay. From left to right, first lane: 2D graph compare the cell responses among the cell models detected at 4000Hz (resistance with SD); second lane: 3D graph of cell responses for WT cells; third lane: 3D graph of cell responses for STRNkd cells; fourth lane: 3D graph of cell responses for STRN3kd cells. The 3D figures indicate cells responses (Z-axis, normalized resistance in ohms) over time (X-axis, hours) and across multiple frequencies (Y-axis, Hz). All resistance detected were normalized with the initial result acquired.

Figure 3B. Cell adhesiveness and migration of MDA MB-361 cells with different STRNs expressions, namely MDA MB-361 WT, MDA MB-361 STRNkd and MDA MB-361 STRN3kd. Top panel: adhesion assay; Bottom panel: migration assay. From left to right, first lane: 2D graph compare the cell responses among the cell models detected at 4000Hz (resistance with SD); second lane: 3D graph of cell responses for WT cells; third lane: 3D graph of cell responses for STRNkd cells; fourth lane: 3D graph of cell responses for STRN3kd cells. The 3D figures indicate cells responses (Z-axis, normalized resistance in ohms) over time (X-axis, hours) and across multiple frequencies (Y-axis, Hz). All resistance detected were normalized with the initial result acquired.

Figure 3C. Cell adhesiveness and migration of MCF7 cells with different STRNs expressions, namely MCF7 WT, MCF7 STRNkd and MCF7 STRN3kd. Top panel: adhesion assay; Bottom panel: migration assay. From left to right, first lane: 2D graph compare the cell responses among the cell models detected at 4000Hz (resistance with SD); second lane: 3D graph of cell responses for WT cells; third lane: 3D graph of cell responses for STRNkd cells; fourth lane: 3D graph of cell responses for STRN3kd cells. The 3D figures indicate cells responses (Z-axis, normalized resistance in ohms) over time (X-axis, hours) and across multiple frequencies (Y-axis, Hz). All resistance detected were normalized with the initial result acquired.

Figure 3D. Cell adhesiveness and migration of SKBR3 cells with different STRNs expressions, namely SKBR3 WT, SKBR3 STRNkd and SKBR3 STRN3kd. Top panel: adhesion assay; Bottom panel: migration assay. From left to right, first lane: 2D graph compare the cell responses among the cell models detected at 4000Hz (resistance with SD); second lane: 3D graph of cell responses for WT cells; third lane: 3D graph of cell responses for STRNkd cells; fourth lane: 3D graph of cell responses for STRN3kd cells. The 3D figures indicate cells responses (Z-axis, normalized resistance in ohms) over time (X-axis, hours) and across multiple frequencies (Y-axis, Hz). All resistance detected were normalized with the initial result acquired.

Figure 4. Matrigel adhesion assay of MDA-MB-231 (up) and MDA-MB-361 (bottom). (A) Representative images of the adhered cells captured at 20X magnification. (B) Bar graphs of the adhered cell number for each cell model (n=12). * $p<0.05$; ** $p<0.01$ for comparisons between the KD and the WT cells.

/Tables

Table-1a. Expression of striatins and STRIPAK partners in mammary tissues and breast cancer tissues of Cardiff cohort.

Category	Subgroup	n=	STRN	STRN3	STRN4	STRIP1	STRIP2	Calmodulin	PPP2CA	PPP2CB	PPP2R1A	PPP2R4
Tissue type	Normal	33	12.05(3.96-35.03)	0.49(0.11-4.21)	85.3(32.4-168.1)	4573(2156-45892)	25857(1662-118966)	3.18(0.72-22.5)	0.3(0.1-3.2)	0(0-3)	1.9(0.6-3.3)	0.00001(0-0.00037)
	Tumour	127	57(14-288) ^a	0.75(0.02-10.09)	84.5(14.9-335.6)	4156(2495-8175)	10232(1750-49386)	5.7(0.4-44.6)	0.5(0.1-3)	1(0-7)	1.58(0.5-4.28)	0.00003(0-0.00027)
Nottingham Prognostic Index (NPI)	Good	68	63(12-254)	0.5(0-12.8)	78.9(4.9-245)	4192(2562-7838)	12908(1728-43916)	2.9(0.1-49.6)	0.6(0.1-4.4)	1(0-46)	1.52(0.5-4)	0.00003(0-0.00029)
	Moderate	38	85(15-866)	0.9(0.1-10)	120(32.3-606.9)	4553(2440-9838)	4761(120-109529)	12(1.8-45.4)	0.22(0.04-7.37)	0.9(0.2-3.1)	1.862(0.409-4.352)	0.00005(0-0.00032)
	Poor	16	49.7(6.6-248.8)	1.07(0.03-13.21)	91.8(33.5-331.8)	3326(1906-15825)	9787(768-213921)	2.62(0.25-17.95)	0.69(0.18-1.35)	0(0-1)	1.869(0.657-3.836)	0.0001(0-0.00018)
Grade	Grade-1	24	25(1-629)	0.16(0-10.13)	50(2-585)	3209(2210-4545)	15580(2221-94997)	2(0-35)	0.3(0.1-4.5)	1.3(0.2-2.7)	0.597(0.121-2.084)	0.00002(0-0.00018)
	Grade-2	43	94(26-557)	0.5(0.1-14.9)	102(10-399)	3708(1673-7023)	9526(411-47310)	2(0.1-52.5)	0.32(0.04-1.68)	1(0-14)	2.101(1.046-5.55) ^d	0.00002(0-0.00014) ^d
	Grade-3	58	49.7(7.1-209.8)	1.1(0.2-7.5)	84.8(35.3-238.2)	6101(2909-16558) ^d	8105(1854-83647)	11.1(1.8-44.6)	0.82(0.11-5.22)	1(0-11)	1.37(0.52-4.32)	0.00007(0-0.00034) ^d
Clinical outcome	Disease free	90	49(7-455)	0.8(0-12.5)	96.8(14.7-357.8)	3914(2577-7390)	12543(2031-68358)	6.3(0.4-46.2)	0.5(0.1-2)	1(0-6)	1.49(0.5-4.02)	0.00002(0-0.00022)
	With Metastasis	7	73.5(25.1-212.5)	0.8(0.16-7.77)	85(55.2-125.2)	2868(1684-6967)	199(31-1972) ^e	5.4(0-55.9)	1.8(0.1-8.2)	1.4(0.4-170.6)	1.88(1.14-9.6)	0.00042(0.00001-0.00067)
	Died of BrCa	16	149(4-667)	0.89(0.04-7.56)	99.9(11.6-463.4)	7150(2466-19400)	8148(701-32499)	10.2(0.8-40.7)	0.18(0.06-2.1)	1(0-8)	2.6(0.5-7.7)	0.00008(0-0.00014)
	All Incidence	28	80.2(32-250.7)	0.77(0.04-6.43)	81.2(28.3-270.2)	5685(1811-9074)	2537(278-29621)	7.5(0.4-44.6)	0.66(0.08-2.87)	1.4(0.2-8.4)	2.1(1.14-7.73)	0.00008(0-0.00031)
Nodal status	Positive	54	55(15-554)	1(0.1-10.2)	119.8(33.2-420.6)	4545(2483-10050)	8127(701-119800)	9.7(0.9-43.2)	0.4(0.08-2.27)	1(0-2)	1.869(0.518-4.237)	0.00005(0-0.0003)
	Negative	68	63(12-254)	0.5(0-12.8)	78.9(4.9-245)	4192(2562-7838)	12908(1728-43916)	2.9(0.1-49.6)	0.6(0.1-4.4)	1(0-46)	1.52(0.5-4)	0.00003(0-0.00029)
ER status	Negative	75	57.4(14.3-287.7)	1(0-10.7)	85(19.6-305.2)	3337(2483-6189)	14070(1868-47039)	11.1(1.5-51.3)	0.5(0.1-4.2)	1(0-8)	1.585(0.525-3.836)	0.00004(0-0.0003)
	Positive	38	59(11-2129)	0.5(0-6.5)	78.9(3.9-493.7)	5055(2528-8209)	6278(793-55289)	2.1(0-17.9) ^f	0.55(0.07-3.8)	1(0-6)	2.1(0.45-6.42)	0.00005(0-0.00014)
Her2	Her2(-)	57	52(7-586)	1.1(0.1-15.1)	102.1(16.4-398.5)	4545(2184-8001)	33053(7107-101396)	5.3(0.5-29.6)	0.8(0.2-3.3)	1(0-6)	1.49(0.48-3.84)	0.00004(0-0.00027)
	Her2(+)	55	81(29-254)	0.75(0.02-7.14)	84.5(13.8-311.9)	3632(2355-8786)	5958(806-30208) ^g	12(0.4-49.1)	0.33(0.08-3.23)	1(0-8)	1.71(0.5-4.51)	0.00002(0-0.00032)

Table-1b. Expression of striatins and STRIPAK partners in mammary tissues and breast cancer tissues of Cardiff cohort.

Category	Subgroup	n=	CCM3	MINK1	MOB4	SIKE1	SLMAP	MST1 (HGFL)	MST1R (RON))	Caveolin	TNKS1	TNKS2
Tissue type	Normal	33	6790(3773-15861)	5948(2561-9834)	20235(9388-25369)	2153(499-3581)	4453(2161-9633)	7(0-412)	0(0-179)	0.164(0.047-0.363)	2.26(0.87-6.03)	0.01(0-0.7)
	Tumour	127	6183(1734-23717)	5525(1996-17477)	19852(7196-38318)	1995(971-4135)	3243(1378-17215)	2(0-349)	0(0-1488)	0.45(0.09-2.49)	5.8(0.5-22.7)	0.01(0-3.22)
Nottingham Prognostic Index (NPI)	Good	68	6832(1827-23843)	5343(1655-16941)	18779(7947-33941)	1907(984-3997)	2904(1252-16639)	0(0-466)	0(0-787)	0.358(0.078-2.14)	1.93(0.31-16.92)	0.09(0-4.55)
	Moderate	38	7508(1284-34305)	6328(2014-28532)	19848(4955-41073)	2499(1338-5834)	4575(1445-17335)	3(0-487)	0(0-160) ^b	0.68(0.12-2.53)	7.9(1-26.7)	0(0-0.9)
	Poor	16	4619(2687-24503)	5678(2431-23419)	31648(16480-42687)	948(463-2884)	9459(3121-44016)	1(0-249)	350(0-41341) ^c	0.78(0.1-7.38)	12(1-44)	0(0-2.57)
Grade	Grade-1	24	3688(1613-13758)	4476(1148-13647)	14373(3902-25883)	2023(1224-5861)	3243(1749-25592)	0(0-135)	0(0-1211)	1.3(0.1-2.7)	3.6(0.2-9.4)	0(0-2.61)
	Grade-2	43	5499(1048-20152)	5905(1348-17857)	18203(5514-33671)	3063(1569-4265)	2603(882-9366)	9(0-737)	0(0-76)	0.597(0.093-2.69)	2.57(0.32-17.71)	0.14(0-4.61)
	Grade-3	58	7049(2832-28673)	5525(2106-21790)	26244(13390-40611)	1601(553-2593)	6690(1772-36975)	0(0-328)	4(0-9011)	0.37(0.08-1.5)	9.9(0.9-36)	0(0-2.95)
Clinical outcome	Disease free	90	5741(1892-24631)	5658(2205-16122)	20591(7196-38318)	2257(1295-3747)	2805(1279-15751)	14(0-494)	0(0-212)	0.47(0.1-2.55)	6.2(0.5-17.7)	0.01(0-3.55)
	With Metastasis	7	3607(734-4230)	4353(2673-5150)	22548(8688-37321)	2800(592-5278)	2802(882-3037)	0(0-777)	0(0-101)	0.05(0.01-0.78)	15.2(3.3-64.2)	0.002(0-0.18)
	Died of BrCa	16	11445(3734-47878)	15408(1529-28364)	35484(18815-41867)	1086(401-5153)	7772(1916-44016)	0(0-51)	9020(0-41341)	0.3(0.03-1.83)	11(1-44)	0.06(0-18.82)
	All Incidence	28	6959(1245-24352)	4379(1909-26160)	31648(10839-41073)	1623(414-4377)	6883(1836-31760)	0(0-51)	39(0-17005) ^e	0.23(0.03-1.83)	11.9(0.9-64.2)	0.01(0-2.57)
Nodal status	Positive	54	6652(1875-24807)	5905(2303-26199)	27954(8118-41469)	2393(1290-4283)	6883(1567-29843)	2(0-320)	1(0-4320)	0.68(0.12-2.63)	9.2(0.9-31)	0(0-1.18)
	Negative	68	6832(1827-23843)	5343(1655-16941)	18779(7947-33941)	1907(984-3997)	2904(1252-16639)	0(0-466)	0(0-787)	0.358(0.078-2.14)	1.93(0.31-16.92)	0.09(0-4.55)
ER status	Negative	75	4667(1908-20436)	5736(2495-16532)	25332(14048-37111)	1823(1290-3090)	2853(1395-14034)	14(0-698)	1(0-2315)	0.31(0.07-1.98)	5.14(0.48-18.42)	0.01(0-3.26)
	Positive	38	7265(1428-24809)	4405(765-21412)	14850(5222-40614)	2084(616-5301)	4351(1306-27238)	0(0-70)	0(0-1005)	0.777(0.173-2.53)	5.3(0.8-23.6)	0.01(0-3.68)
Her2	Her2(-)	57	4817(1899-24173)	6116(3052-16218)	20591(11843-36248)	2522(984-5112)	3690(1388-17456)	9(0-447)	0(0-1312)	0.75(0.1-2.17)	1.5(0.3-18.4)	0.01(0-3.89)
	Her2(+)	55	7472(1657-25436)	4379(1491-20523)	19852(6181-39955)	1826(744-3734)	3093(1333-19952)	0(0-296)	0(0-2165)	0.36(0.07-1.83)	8.3(1.3-39)	0(0-3.36) ^g

Note: Shown are Median (interquartile range). Mann-Whitney U tests were conducted and statistical significance was reached by comparing between the groups. ^a p<0.05 vs normal; ^b p<0.05 vs good prognosis; ^c p<0.05 vs moderate prognosis; ^d p<0.05 vs Grade-1; ^e p<0.05 vs disease free; ^f p<0.05 vs ER negative; ^g p<0.05 vs Her2 negative;

Table-2. STRIPAK and patients' OS and DFS, Cardiff data by Cox Regression

	OS		DFS	
	P value	HR	P value	HR
STRN	0.434	1.804 (0.411-7.918)	0.260	2.306 (0.539-9.871)
STRN3	0.178	2.031 (0.724-5.700)	0.384	1.465 (0.621-3.456)
STRN4	0.196	3.789 (0.504-28.492)	0.248	2.352 (0.551-10.038)
STRIP1	0.053	3.018 (0.984-9.254)	0.249	1.853 (0.649-5.292)
STRIP2	0.014	4.388 (1.349-14.267)	0.265	1.781 (0.646-4.913)
Calmodulin	0.019	4.384 (1.269-15.149)	0.055	2.489 (0.981-6.316)
PPP2CA	0.063	0.414 (0.163-1.050)	0.069	0.468 (0.206-1.061)
PPP2CB	0.110	0.471 (0.187-1.186)	0.105	0.509 (0.224-1.153)
PPP2R1A	0.079	0.436 (0.173-1.100)	0.073	0.473 (0.208-1.073)
PPP2R4	0.590	1.292 (0.509-3.278)	0.752	1.141 (0.503-2.589)
CCM3	0.032	4.003 (1.128-14.205)	0.488	1.381 (0.555-3.437)
MINK1	0.011	3.749 (1.356-10.361)	0.146	2.053 (0.779-5.410)
MOB4	0.010	4.598 (1.441-14.676)	0.075	2.460 (0.915-6.613)
SIKE1	0.115	3.056 (0.763-12.246)	0.136	2.467 (0.752-8.086)
SLAMP	0.035	3.496 (1.093-11.176)	0.178	2.033 (0.723-5.714)
MST1 (HGFL)	0.441	0.646 (0.213-1.964)	0.358	0.628 (0.233-1.693)
MST1R (RON)	0.415	1.473 (0.581-3.735)	0.285	1.569 (0.687-3.580)
Caveolin	0.674	0.816 (0.315-2.110)	0.303	0.648 (0.283-1.481)
TNKS1	0.093	5.666 (0.748-42.94)	0.054	7.253 (0.970-54.222)
TNKS2	0.261	1.854 (0.633-5.431)	0.692	1.194 (0.497-2.870)

Table-3. Univariate and multivariate analysis of the STRIPAK signature and clinical factors against overall survival (Cox Regression)

Factors tested		Univariate		Multivariate	
		HR (95%CI)	P value	HR (95%CI)	P value
STRN/STRIPAK signature		1.203 (1.095-1.322)	<0.001	1.284 (1.127-1.463)	<0.001
Clinical factors	NPI	2.874 (1.579-5.230)	0.001	2.582 (0.654-10.198)	0.176
	Grade	1.121 (0.821-1.530)	0.472	1.503 (0.756-2.985)	0.245
	Staging	1.269 (0.897-1.796)	0.178	1.331 (0.800-2.215)	0.271
	Nodal status	4.688 (1.575-14.557)	0.006	0.602 (0.060-6.006)	0.666
	ER	2.375 (0.818-6.896)	0.112	2.647 (0.785-8.930)	0.117
	Her2	3.181 (1.010-10.022)	0.048	4.682 (1.274-17.208)	0.020
Receptor subtypes	TNBC	2.417 (0.858-6.810)	0.095	0.383 (0.042-3.513)	0.396
	ER(+)/Her2(-)	2.631 (0.981-7.059)	0.055	2.119 (0.274-16.358)	0.472
	ER(-)/Her2(+)	2.871 (1.110-7.247)	0.030	4.537 (0.592-34.756)	0.145
	ER(+)/Her2(+)	2.123 (1.202-3.749)	0.010	1.435 (0.474-4.346)	0.522

Table-4a. Patient's DRUG response, tumour pathological responses to chemotherapies*.

Molecule	Response status	Number	Transcript expression level		ROS	
			Median (Min-Max)	P value	AUC	P value
STRN3	Responders	532	428 (4-2480)	0.00002	0.565	0.000015
	Non-Responders	1100	342 (6-3394)			
STRN4	Responders	532	191 (9-1068)	1e-17	0.631	0e+00
	Non-Responders	1100	314 (6-1460)			
STRIP1 (FAM40A)	Responders	119	464 (105-1057)	0.34	0.529	0.18
	Non-Responders	388	436 (50-1339)			
STRIP2 (FAM40B)	Responders	119	54 (2-819)	0.30	0.531	0.15
	Non-Responders	388	47 (0-855)			
Calmodulin	Responders	532	1696 (52-7615)	0.15	0.522	0.076
	Non-Responders	1100	1547 (23-10294)			
SIKE1	Responders	119	452 (24-1382)	0.17	0.542	0.073
	Non-Responders	388	504 (5-4356)			
MINK1	Responders	532	1062 (285-9626)	0.53	0.51	0.26
	Non-Responders	1100	1098 (72-14670)			
CCM3 (PDCD10)	Responders	532	3443 (7-13811)	8.6e-09	0.588	3.5e-09
	Non-Responders	1100	2876 (15-13752)			
MOB4B (MOBKL1B)	Responders	532	1287 (48-5356)	0.85	0.503	0.42
	Non-Responders	1100	1270 (21-6644)			
MOB4A (MOBKL1A)	Responders	119	1255 (163-3290)	0.06	0.557	0.031
	Non-Responders	388	1097 (70-5515)			
PPP2R1A	Responders	532	538 (25-3238)	5.8e-15	0.619	3.4e-15
	Non-Responders	1100	1150 (35-4831)			
PPP2CA	Responders	532	2268 (241-5931)	0.016	0.537	0.0076
	Non-Responders	1100	2031 (87-6764)			
PPP2CB	Responders	532	2990 (195-10822)	0.00013	0.558	0.000078
	Non-Responders	1100	1510 (25-12568)			
MST1R	Responders	532	265 (10-1611)	4.1e-11	0.601	4.4e-12
	Non-Responders	1100	342 (19-1774)			
PPP2R4	Responders	532	659 (150-3102)	2.2e-21	0.645	<0.0000indef
	Non-Responders	1100	904 (99-5432)			
Caveolin	Responders	532	1542 (12-24193)	27.4e-7	0.575	3.5e-7
	Non-Responders	1100	974 (3-22206)			
TNKS2	Responders	532	866 (3-4463)	21.3e-17	0.630	<0.0000indef
	Non-Responders	1100	532 (9-2929)			

* from ROCplot.com (45).

Table-4b. Patient's DRUG response, 5-year RFS response to chemotherapies*

Molecule	Response status	n=	Transcript expression level		ROC	
			Median (Min-Max)	P value	AUC	P value
STRN3	Responders	256	451 (15-2923)	0.00099	0.587	0.00039
	Non-Responders	220	362 (32-2391)			
STRN4	Responders	256	424(107-1411)	0.42	0.521	0.21
	Non-Responders	220	393 (101-1785)			
STRIP1 (FAM40A)	Responders	115	444 (141-806)	0.78	0.514	0.39
	Non-Responders	48	411 (243-744)			
STRIP2 (FAM40B)	Responders	115	46 (1-1234)	0.074	0.589	0.042
	Non-Responders	48	34 (2-180)			
Calmodulin	Responders	256	1759 (488-6555)	0.2	0.534	0.097
	Non-Responders	220	1660 (463-5411)			
SIKE1	Responders	115	393 (5-1225)	0.0033	0.646	0.0011
	Non-Responders	48	500 (38-1027)			
MINK1	Responders	256	1169 (267-5696)	0.30	0.528	0.15
	Non-Responders	220	1266 (312-3739)			
CCM3 (PDCD10)	Responders	256	2982 (428-12107)	0.73	0.509	0.37
	Non-Responders	220	2990 (570-11370)			
MOB4B (MOBKL1B)	Responders	532	1160 (347-3723)	0.091	0.545	0.044
	Non-Responders	256	1268 (431-3500)			
MOB4A (MOBKL1A)	Responders	220	596 (116-3018)	0.81	0.512	0.40
	Non-Responders	48	563 (248-1404)			
PPP2R1A	Responders	256	1370 (348-3557)	0.80	0.507	0.40
	Non-Responders	220	1334 (420-3058)			
PPP2CA	Responders	256	2394 (665-5597)	0.00021	0.598	0.000085
	Non-Responders	220	1994 (241-5705)			
PPP2CB	Responders	256	3030 (339-11837)	0.0026	0.579	0.0013
	Non-Responders	220	2577 (785-10412)			
MST1R	Responders	256	360 (16-2343)	0.014	0.565	0.0066
	Non-Responders	220	418 (25-1351)			
PPP2R4	Responders	256	1106 (299-3980)	0.09	0.545	0.044
	Non-Responders	220	1018 (317-3727)			
Caveolin	Responders	256	1097 (15-8858)	0.21	0.533	0.11
	Non-Responders	220	16 (12599)			
TNKS2	Responders	256	798 (65-2913)	0.0068	0.572	0.0032
	Non-Responders	220	640 (114-2098))			

* from ROCplot.com (45)

Table-5. STRN3 transcript expression level and patients' response to chemotherapies in subtypes of breast cancer (* by Mann-Whitney U test)[#]

Hormone receptor and subtypes		Pathological response			5-year RFS response				
		Response status	Number	Median (Min-Max)	P value	Response status	Number	Median (Min-Max)	P value
ER status	ER (-)	Responders	279	338 (15-2480)	0.70	Responders	115	446 (15-2014)	0.12
		Non-Responders	387	351 (32-3394)		Non-Responders	111	360 (32-2391)	
	ER (+)	Responders	253	517 (4-1927)	1.4e-10	Responders	141	454 (16-2923)	0.0025
		Non-Responders	713	338 (6-3160)		Non-Responders	109	363 (85-1092)	
Her2 status	Her2 (-)	Responders	389	505 (4-2480)	6.2e-12	Responders	183	409 (15-1610)	0.0043
		Non-Responders	890	336 (6-3160)		Non-Responders	173	331 (32-1104)	
	Her2 (+)	Responders	143	301 (64-2190)	0.0014	Responders	73	593 (133-2923)	0.31
		Non-Responders	210	404 (18-3394)		Non-Responders	47	549 (153-2391)	
ER/Her2 status subtypes	ER(-)/Her2(+)	Responders	83	304 (64-2190)	0.0034	Responders	35	655 (133-2014)	0.69
		Non-Responders	110	419 (106-3394)		Non-Responders	26	580 (161-2391)	
	ER(+)/Her2(-)	Responders	193	720 (4-1927)	2.3e-16	Responders	103	409 (16-1349)	0.017
		Non-Responders	613	334 (6-3160)		Non-Responders	88	336 (85-1092)	
	ER(+)/Her2(+)	Responders	60	288 (76-1564)	0.053	Responders	38	579 (216-2923)	0.1
		Non-Responders	100	364 (18-2645)		Non-Responders	21	512 (153-957)	
	TNBC	Responders	196	428 (15-2480)	0.14	Responders	80	413 (15-1610)	0.13
		Non-Responders	277	339 (32-2180)		Non-Responders	84	328 (32-1104)	

* from ROCplot.com (45).

Table-6. IC50 of chemo-drugs tests

	MDA MB-231/WT	MDA MB-231/STRNkd	MDA MB-231/STRN3kd
Paclitaxel	58.6nM	167nM	279nM
Docetaxel	24.3nM	31.9nM	32,2nM
	MDA MB-361/WT	MDA MB-361/STRNkd	MDA MB-361/STRN3kd
Paclitaxel	14nM	19nM	14.2nM
Docetaxel	5.23nM	0.8nM	5.29nM
	MCF7/WT	MCF7/STRNkd	MCF7/STRN3kd
Paclitaxel	4.74nM	0.726nM	2.69nM
Docetaxel	0.95nM	0.55nM	6.5nM
	SKBR3/WT	SKBR3/STRNkd	SKBR3/STRN3kd
Paclitaxel	7.34nM	0.12nM	9.03nM
Docetaxel	4.9nM	13.63nM	0.39nM

Supplement-1. PCR primers

Molecule	Forward (5'-3')	Reverse (5'-3') *
STRIP1	tgctttgaggaggacttc	<u>actgaacctgaccgtacag</u> acttccaagccatccag
STRIP2	gtatggagatgcagatggg	<u>actgaacctgaccgtaca</u> cttcaaagcacctcctgt
MOB4	tatggtcatggcggagg	<u>actgaacctgaccgtacaca</u> aaggattcatcaggcca
CCM3 (PDCD10)	ccatggtttctatgcccc	<u>actgaacctgaccgtaca</u> cttgatgaagcggtct
SIKE1	gagtcgctggtggatca	<u>actgaacctgaccgtacag</u> tccttcatatcgatgca
MINK1	cctactacggagccttca	<u>actgaacctgaccgtaca</u> taggcgatacagtcctcc
SLMAP	tggagtagacgtgacaga	<u>actgaacctgaccgtacag</u> ggcttccataccatctg
STRN3	actgggagggtggaacg,	<u>actgaacctgaccgtaca</u> tccttcttcagggttctcttg
STRN	ggaaacaaggtcgacaact	<u>actgaacctgaccgtaca</u> cgactcgttttagatttca
STRN4	ggtcacctggagaaca	<u>actgaacctgaccgtacag</u> tctgtgtagccacctct
PPP2CA	ggagattatgttgacagagga	<u>actgaacctgaccgtaca</u> ctcgaagaatggtgatgc
PPP2CB	gagactgtgactcttctgt	<u>actgaacctgaccgtaca</u> cggcttctcgtgatttct
PPP2R1A	ggcaaagacaacaccatc	<u>actgaacctgaccgtaca</u> cgttcacacagtcagggt
PPP2R4	tccacacagttccagaca	<u>actgaacctgaccgtaca</u> actcgaaggtagcttct
MST1 (HGFL)	gaccagccgcatcaatc	<u>actgaacctgaccgtaca</u> cttggaaacccgctgac
MST1R (RON)	catccaccagtgccaac	<u>actgaacctgaccgtaca</u> ccacacagtcagccacag
TNKS1	cctttccctcactcgat	<u>actgaacctgaccgtaca</u> ccaccgagtcactgtctt
TNKS2	ctggtgacgcctgagaag	<u>actgaacctgaccgtacag</u> tctttccgccccaaacc,
Caveolin	<u>actgaacctgaccgtaca</u> aaca cgtagctgccttc	cttgtagatgttgcctgtt
GAPDH	aaggtcatccatgacaactt	<u>actgaacctgaccgtaca</u> gcatccacagtcctctg
CK19	agccactactacagacat	<u>actgaacctgaccgtaca</u> tcgatctgcaggacaatc

* Z-sequence for QPCR analysis